



### 저작자표시-비영리-변경금지 2.0 대한민국

이용자는 아래의 조건을 따르는 경우에 한하여 자유롭게

- 이 저작물을 복제, 배포, 전송, 전시, 공연 및 방송할 수 있습니다.

다음과 같은 조건을 따라야 합니다:



저작자표시. 귀하는 원 저작자를 표시하여야 합니다.



비영리. 귀하는 이 저작물을 영리 목적으로 이용할 수 없습니다.



변경금지. 귀하는 이 저작물을 개작, 변형 또는 가공할 수 없습니다.

- 귀하는, 이 저작물의 재이용이나 배포의 경우, 이 저작물에 적용된 이용허락조건을 명확하게 나타내어야 합니다.
- 저작권자로부터 별도의 허가를 받으면 이러한 조건들은 적용되지 않습니다.

저작권법에 따른 이용자의 권리와 책임은 위의 내용에 의하여 영향을 받지 않습니다.

이것은 [이용허락규약\(Legal Code\)](#)을 이해하기 쉽게 요약한 것입니다.

[Disclaimer](#)



**Comprehensive Analysis of the Influence of  
Preparation design based on Total Occlusal  
Convergence, Margin shape, Crown height, and  
Auxiliary groove on Stress distribution and  
Stability of Full-coverage crown in the posterior  
area. A Finite Element Analysis and In-Vitro Study**

**Yuwon Jeong**

**The Graduate School**

**Yonsei University**

**Department of Prosthodontics**

**Comprehensive Analysis of the Influence of  
Preparation design based on Total Occlusal  
Convergence, Margin shape, Crown height, and  
Auxiliary groove on Stress distribution and  
Stability of Full-coverage crown in the posterior  
area. A Finite Element Analysis and In-Vitro Study**

**A Dissertation Thesis**

**Submitted to the Department of Prosthodontics and the Graduate  
School of Yonsei University in partial fulfillment of the requirements  
for the degree of Doctor of Philosophy in Prosthodonticsii**

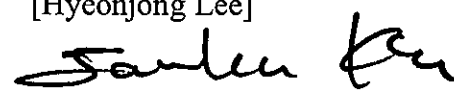
**Yuwon Jeong**

**December 2024**

**This certifies that the Dissertation  
of [Yuwon Jeong] is approved.**



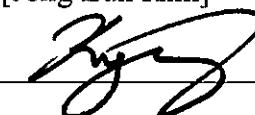
Thesis Supervisor [Hyeonjong Lee]



Thesis Committee Member [Jee Hwan Kim]



Thesis Committee Member [Jong Eun Kim]



Thesis Committee Member [Kyung Chul Oh]



Thesis Committee Member [Jae Hyun Lee]

**The Graduate School  
Yonsei University  
December, 2024**



## **DEDICATION**

To God, for His guidance and blessings.

To my family and forever partner, for your constant love and support.

## TABLE OF CONTENTS

ABSTRACT .....	viii
1. Introduction .....	1
2. Materials and Methods .....	3
2.1. Finite Element Analysis (FEA) .....	5
2.1.1. Sketch design .....	5
2.1.2. Creation of Solid models .....	9
2.1.3. Material properties .....	14
2.1.4. Meshing .....	15
2.1.5. Boundary and Contact conditions .....	16
2.1.6. Loading conditions .....	17
2.1.7. Simulation .....	19
2.2. In-vitro study specimen design .....	19
2.3. Statistical analysis .....	22
3. Results .....	23
3.1. Finite Element Analysis Overall Results .....	23
3.1.1. Crown height (3mm, 4.5mm, and 6mm) .....	23
3.1.2. Finish line (Chamfer, Deep chamfer, and Vertical) .....	25
3.1.3. Auxiliary groove (Mesial groove) .....	29
3.2. Von stress values (MPa) on the tooth structure .....	32
3.2.1. Crown height (3mm, 4.5mm, and 6mm) .....	32
3.2.2. Finish line (Chamfer, Deep chamfer, and Vertical) .....	33

3.2.3. Auxiliary groove (Mesial groove).....	34
3.3. Von stress values (MPa) on the cement layer .....	35
3.3.1. Crown height (3mm, 4.5mm, and 6mm).....	35
3.3.2. Finish line (Chamfer, Deep chamfer, and Vertical).....	37
3.3.3. Auxiliary groove (Mesial groove).....	39
3.4. In-vitro Study Results .....	42
3.4.1. Pull-out test .....	42
3.4.2. Occlusal loading + Pull-out test after 30° oblique loading .....	47
4. Discussion .....	52
4.1. Finite Element Analysis .....	52
4.2. In-Vitro Study results.....	54
4.3. Correlations between FEA and In-Vitro Study .....	55
5. Conclusions.....	61
6. References.....	62
Abstract in Korean .....	67

## LIST OF FIGURES

Figure 1. Step by step of Finite Element Analysis.....	5
Figure 2. Sketch design of Finite Element Analysis. A. Sketch of crown, tooth structure, cement layer, periodontal ligament (PDL), cancellous bone, and cortical bone. Edges were rounded and margin was extended to minimize mesh erroring in further simulation. TOC angulation was applied regarding to each total occlusal convergence (TOC). B. Amplified visualization of cement layer, an offset of 0.1mm (100microns) was performed from the prepared tooth.....	6
Figure 3. Sketch design of this study. A-C: Margin design: Chamfer, Deep chamfer, and Vertical. D-F: Crown height: 3mm, 4.5mm, and 6mm. G-I: TOC: 10°, 20°, and 30° .....	8
Figure 4. Solid bodies of resin cement layer, tooth structure, PDL, cancellous bone and cortical bone.....	9
Figure 5. Anatomical modifications were made to mimic a mandibular first right molar.....	10
Figure 6. Three-dimensional Finite Element solid models. A. Crown height of 3mm, Chamfer finish line, TOC 10°, 20°, and 30°, presence of margin parallelism of 1mm at TOC 20° and 30°. B. Crown height of 4.5mm, Chamfer finish line, TOC 10°, 20°, and 30°, presence of margin parallelism of 1mm at TOC 20° and 30°. C. Crown height of 4.5mm, Deep chamfer finish line, TOC 10°, 20°, and 30°, presence of margin parallelism of 1mm at TOC 20° and 30°. *TOC: Total Occlusal Convergence.....	11
Figure 7. Three-dimensional Finite Element solid models. A. Crown height of 4.5mm, Vertical finish line, TOC 10°, 20°, and 30°, presence of margin parallelism of 1mm at TOC 20° and 30°. B. Crown height of 4.5mm, Chamfer finish line, TOC 10°, 20°, and 30°, presence of margin parallelism of 1mm at TOC 20° and 30°, presence of auxiliary mesial groove. C. Crown	

height of 6mm, Chamfer finish line, TOC 10°, 20°, and 30°, presence of margin parallelism of 1mm at TOC 20° and 30°. *TOC: Total Occlusal Convergence .....	12
Figure 8. Three-dimensional Finite Element solid model of Auxiliary Mesial Groove. A. Internal surface of crown. B. Occlusal view of tooth structure. C. Internal surface of cement layer.....	14
Figure 9. The tetrahedral mesh of finite elements. A. Overall view of mesh. B. The cement layer has a finer mesh size than other components. C. Amplified view of mesh form.....	16
Figure 10. Structural constraints fixed at cancellous bone and cortical bone. A. Model view of constraints. B. Constraints remain fixed at loading force application. ....	17
Figure 11. Loading parameters used in this study for Finite Element Analysis. 200N of force was applied. A. Vertical loading at occlusal surface. Load case 1: buccal cusps. Load case 2: central fossa. Load case 3: buccal cusps and central fossa. B. Oblique loading at occlusal surface (Angulation of 30 degrees). Load case 1: Slightly below buccal cusps. Load case 2: Slightly below lingual cusps. Load case 3: slightly below buccal and lingual cusps. ....	17
Figure 12. Reference points in the occlusal surface of the crown. A. Vertical loading cases. B. Oblique loading cases.....	18
Figure 13. Description of In-vitro study. ....	20
Figure 14. Modifications of each crown and preparation design for the in-vitro study. A. Pull-out test experiment design. B. Occlusal loading + Pull-out test experiment design.....	21
Figure 15. In-vitro study conducted using a Universal Testing Machine (UTM, Instron). A. pull-out test setup utilizing a 0.7 mm orthodontic wire to apply	

force. B. (a) Initial occlusal loading test performed using a plane incorporated on the occlusal surface of the crown. (b) Subsequent pull-out test conducted with dental floss to facilitate separation. ....	22
Figure 16. Bucco-lingual sectional view of Finite Element Analysis of load cases 4, 5, and 6 from Crown height group (Finish line: Chamfer / TOC: 30°) ..	25
Figure 17. Bucco-lingual sectional view of Finite Element Analysis of load cases 4, 5, and 6 from Finish line group. (Crown height: 4.5mm / TOC: 30°) ....	28
Figure 18. Bucco-lingual sectional view of Finite Element Analysis of load cases 4, 5, and 6 between Auxiliary mesial groove and No groove. (Crown height: 4.5mm / TOC: 30°/ Finish line: Chamfer).....	30
Figure 19. Cement layer view of Finite Element Analysis of load cases 4, 5, and 6 from Crown height group (Finish line: Chamfer/TOC:30°) .....	37
Figure 20. Cement layer view of Finite Element Analysis of load cases 4, 5, and 6 from Finish line group (Crown height:4.5mm/TOC:30°).....	39
Figure 21. Finite Element Analysis results on cement layer of load cases 4, 5, and 6 from between groups 'No groove' and 'Mesial groove'. (Crown height: 4.5mm/ TOC:30°).....	41
Figure 22. Pull-out test results (N) of Study group TOC. No statistical significance was found among the tested groups.....	43
Figure 23. Pull-out test results (N) of Study group Finish line (Chamfer, Deep chamfer, Vertical). No statistical significance was found among the tested groups. ....	44
Figure 24. Pull-out test results (N) of Study group Auxiliary groove. Statistical significance was found from No Groove (NG) group from groups MG (Mesial groove) and MG+MP (Mesial groove + Margin parallelism of 1mm). ....	45

Figure 25. Pull-out test results (N) of Study group Crown height. Statistical significance was found from crown height 3mm compared to crown heights 4.5mm and 6mm.....	46
Figure 26. Occlusal loading test results (N) of Study group TOC. Statistical significance was found among the tested groups.....	48
Figure 27. Occlusal loading test results (N) of Study group Finish line. Statistical significance was found from Deep chamfer group compared to groups Chamfer and Vertical.....	49
Figure 28. Occlusal loading test results (N) of Study group Auxiliary groove. Statistical significance was found from No Groove (NG) group from groups MG (Mesial groove) and MG+MP (Mesial groove + Margin parallelism of 1mm).....	50
Figure 29. Occlusal loading test results (N) of Study group Crown height. Statistical significance was found among the tested groups.....	51
Figure 30. Finite element analysis (FEA) and Pull-out test results A.FEA results of von mises stress values at cement layer comparing the addition of 1mm of margin parallel at TOC of 20° and 30°. (Finish line: Chamfer). B. Buccolingual sectional view of Load case 5 on different crown heights at different TOC. (Finish line: Chamfer).....	56
Figure 31. Visualization of force direction of each load case.....	58
Figure 32. Stress distribution within oblique loading cases. ....	58

## LIST OF TABLES

Table 1. Finite Element Analysis and In-Vitro study groups .....	3
Table 2. Mechanical properties of materials used in finite element analysis.....	14
Table 3. Mesh setting of finite elements used in this study. ....	15
Table 4. Von mises stress values (MPa) of study group ‘Crown height’ .....	24
Table 5. Von mises stress values (MPa) of study group ‘Finish line’ .....	26
Table 6. Von mises stress values (MPa) of study group ‘Auxiliary groove’ .....	29
Table 7. Comprehensive FEA stress of crown based on multiple design factors in Load case 5 .....	31
Table 8. Finite element analysis maximum stress values (MPa) of the cement layer of Crown height group.....	36
Table 9. Finite element analysis maximum stress values (MPa) of the cement layer of Finish line group.....	37
Table 10. Finite element analysis maximum stress values (MPa) of the cement layer of auxiliary mesial groove. ....	40
Table 11. Comprehensive FEA stress of cement layer based on multiple design factors in Load case 5.....	41
Table 12. Pull-out test results of In-vitro study .....	42
Table 13. Occlusal loading and Pull-out test results of In-vitro study .....	47

## ABSTRACT

Comprehensive analysis of the influence of preparation design based on Total Occlusal Convergence, Margin shape, Crown height, and Auxiliary groove on stress distribution and stability of Full-coverage crown in the posterior area. A Finite Element Analysis and In-Vitro Study.

**Purpose:** The purpose of this study was to evaluate the influence of tooth preparation design factors such as total occlusal convergence (TOC), finish line design, crown height, auxiliary grooves, margin parallelism, and diverse loading direction on the stress distribution and stability of mandibular full-coverage crowns using both finite element analysis (FEA) and in vitro testing.

**Methods:** A three-dimensional finite element analysis (FEA) model of a monolithic zirconia crown was developed based on a mandibular first molar. Tooth preparation designs varied by three crown heights, three types of finish line, presence of auxiliary grooves and marginal parallelism, and four different TOC, resulting in 35 different preparations. Multiple loading directions, both vertical and oblique, were simulated at a force of 200N. Select groups underwent in-vitro testing to validate FEA results, using a universal testing machine (UTM) to assess pull-out and occlusal loading strengths. Statistical analysis was performed, with significance set at  $p<0.05$ .

**Results:** The finite element analysis revealed that increasing the TOC and crown height significantly impacted stress distribution. Stress values ranged from 471 MPa to 3617 MPa, with higher stress observed at 30° TOC, especially under oblique loading. The addition of a 1mm margin parallel (MP) reduced stress at higher TOC. Chamfer finish lines demonstrated the best mechanical performance, showing the lowest stress levels, while deep chamfer and vertical finish lines generated higher stress concentrations. The presence of auxiliary mesial grooves and taller crowns improved pull-out strength and reduced stress

levels, especially at higher TOC. In-vitro testing corroborated these findings, demonstrating that the addition of MP and grooves enhance retention and reduce stress under both occlusal load and pull-out strength.

**Conclusions:** Tooth preparation design factors, including TOC, finish line design, crown height, marginal parallelism, and auxiliary grooves, play crucial roles in optimizing stress distribution and mechanical performance of full-coverage crowns in the posterior area. The modification of preparation design by adding 1mm of margin parallel (MP) mitigates stress at higher TOC, and chamfer finish lines, and taller crowns improve crown retention and strength. Auxiliary grooves further reduce stress at higher TOC.

**Key words:** Digital dentistry, 3D evaluation, finite element analysis, tooth preparation design, full-coverage crown

## 1. Introduction

Full-coverage restorations represent a routine treatment modality employed by dental practitioners to restore compromised teeth. These restorations consist of the definitive crown, the remaining natural tooth structure, and a cement layer that fills the internal gap between the restoration and the prepared tooth structure. Given the prevalence of this treatment, numerous investigations have been conducted to evaluate the long-term survival and effectiveness of full-coverage restorations.

Full-coverage crowns are typically indicated where a significant portion of the tooth structure has been compromised (Christensen 2007, Suksaphar et al. 2017). The survival of these crowns is well-documented to be highly related to the type of restorative material used, as well as the preparation design, crown design, and manufacturing methods, all of which can significantly affect the mechanical behavior of the final restoration (Goodacre et al. 2001, Pjetursson et al. 2015, Goodacre et al. 2023, Sailer et al. 2023, Suksuphan et al. 2024, Alnajjar et al. 2024).

The design of tooth preparation may vary based on the restorative material utilized; however, the fundamental principles governing tooth preparation have remained relatively consistent over time (Goodacre et al. 2001, Podhorsky et al. 2015). Regardless of the material selected, optimal parameters for tooth preparation prioritize the preservation of remaining tooth structure while ensuring adequate space for the restoration (Tiu et al. 2015, Schriwer et al. 2017). An ideal preparation design must therefore provide sufficient retention and resistance to ensure the longevity and effectiveness of the restoration.

Key parameters influencing tooth preparation include the total occlusal convergence angle (TOC), type of finish line, and the crown length (McCracken et al. 2016). Many in vitro studies have been conducted and demonstrated that finish line design can influence fracture resistance of final restoration (Findakly et al. 2019, Abdulazeez et al. 2022, Kumar et al. 2022, Ashour et al. 2024). Furthermore, TOC of tooth preparation can influence directly the internal adaptation of complete crowns (Mou et al. 2002, Zidan and Ferguson 2003, Vinnakota et al. 2015, Schriwer et al. 2021).

Additionally, crown heights can also influence the retention of the restoration. The minimal occlusal-cervical height should be 2mm to achieve adequate retention of posterior crown (Jing et al. 2019). It has been demonstrated that the addition of auxiliary grooves on compromised molar preparation enhances the resistance to dislodgments of crown (Lu et al. 2008). The addition of auxiliary grooves in the axial walls can provide additional core thickness in oblique loading cases (Qasim et al. 2018).

Previous research has demonstrated a direct correlation between tooth preparation design and the longevity of dental restorations. However, most of these studies have been limited in scope, often examining only a narrow range of preparation designs through Finite Element Analysis (FEA) or in-vitro methods, typically employing a single loading parameter (Baladhandayutham et al. 2015, Skjold et al. 2019, Cárdenas et al. 2022).

The continuous advancements in computational technology have significantly enhanced the capabilities and accuracy of FEA, allowing for more precise simulations and analyses. Previous studies using FEA have demonstrated the critical role of preparation design in optimizing crown performance (Zarone et al. 2005, Motta et al. 2014, Maghami et al. 2018, Zheng et al. 2022). In the realm of dentistry, FEA has emerged as an essential method for understanding the complex interactions between dental materials, tooth structures, and applied forces. A pioneering study by Hojjatie and Anusavice in 1990 marked a significant advancement in this area, as they employed FEA to investigate stress distribution within dental crowns.

The integration of FEA with in vitro studies offers a robust methodology for evaluating the mechanical performance of dental crowns. While FEA provides a theoretical framework for predicting stress distribution and identifying potential failure points, in vitro studies validate these predictions through controlled experimentation. This combined approach enables a more comprehensive understanding of how preparation design and loading forces interact.

The present study seeks to address the limitations of previous research by evaluating an extensive array of preparation designs under diverse loading scenarios to better simulate real clinical conditions. Using FEA, this study simulates diverse loading directions on the

occlusal surface to identify preparation designs that optimize stress distribution and minimize the risk of crown failure. Additionally, in vitro experiments were conducted to validate the FEA findings, ensuring that the results are both theoretically and clinically relevant.

The purpose of this study was to evaluate the influence of different tooth preparation designs on the stress distribution and stability of a full-coverage crown in the posterior region. By employing both FEA and in vitro methodologies, this research aims to provide a comprehensive understanding of how preparation parameters and loading conditions affect the stress distribution and stability of dental crowns. The null hypothesis of this study is that no influence was found among different preparation designs and loading parameters on the stress distribution and stability of full-coverage crown.

## 2. Materials and Methods

The study focused on evaluating different preparation designs, categorized based on crown height, finish line, presence of auxiliary groove, margin parallelism and total occlusal convergence (TOC). In addition, diverse loading conditions were evaluated in FEA. The study groups of this study were divided into finite element analysis (FEA) and in vitro studies (Table 1). The FEA study groups were assessed using tooth preparation parameters such as crown height, finish line, auxiliary grooves, total occlusal convergence (TOC) and 1mm of margin parallelism (MP), using diverse loading conditions. The In-vitro study groups were meticulously selected following the completion of the FEA. The study groups were assessed based on several key parameters, including TOC, finish line design, the presence of auxiliary grooves, and crown height.

Table 1. Finite Element Analysis and In-Vitro study groups

<b>Finite Element Analysis (n=30)</b>	<b>In-Vitro (n=13)</b>
3mm-Chamfer-10°	<b>Study 1</b>
3mm-Chamfer-20°	4.5mm-Chamfer-20°
3mm-Chamfer-30°	4.5mm-Chamfer-30°
3mm-Chamfer-20°-MP	4.5mm-Chamfer-20°-MP

3mm-Chamfer-30°-MP	4.5mm-Chamfer-30°-MP
4.5mm-Chamfer-10°	<b>Study 2</b>
4.5mm-Chamfer-20°	4.5mm-Chamfer-10°
4.5mm-Chamfer-30°	4.5mm-DeepChamfer-10°
4.5mm-Chamfer-20°-MP	4.5mm-Vertical-10°
4.5mm-Chamfer-30°-MP	<b>Study 3</b>
4.5mm-Chamfer-10°-MG	3mm-Chamfer-30°
4.5mm-Chamfer-20°-MG	4.5mm-Chamfer-30°-MG
4.5mm-Chamfer-30°-MG	4.5mm-Chamfer-30°-MP-MG
4.5mm-Chamfer-20°-MP-MG	<b>Study 4</b>
4.5mm-Chamfer-30°-MP-MG	3mm-Chamfer-20°
4.5mm-DeepChamfer-10°	4.5mm-Chamfer-20°
4.5mm-DeepChamfer-20°	6mm-Chamfer-20°
4.5mm-DeepChamfer-30°	
4.5mm-DeepChamfer-20°-MP	
4.5mm-DeepChamfer-30°-MP	
4.5mm-Vertical-10°	
4.5mm-Vertical-20°	
4.5mm-Vertical-30°	
4.5mm-Vertical-20°-MP	
4.5mm-Vertical-30°-MP	
6mm-Chamfer-10°	
6mm-Chamfer-20°	
6mm-Chamfer-30°	
6mm-Chamfer-20°-MP	
6mm-Chamfer-30°-MP	

\*Labelling order: Crown height – Finish line design – Total Occlusal Convergence – Presence of Margin parallelism of 1mm (MP) – Presence of Auxiliary mesial groove (MG)

## 2.1. Finite Element Analysis (FEA)

The creation of the 3D model for FEA was performed using advanced 3D CAD modeling software, specifically Fusion 360 (Autodesk, San Francisco, California). This software provides a robust platform for designing intricate geometry and simulating mechanical behaviors, making it an ideal choice for our modeling needs. Figure 1 illustrates the step-by-step process of FEA. The following is a detailed description of each step.

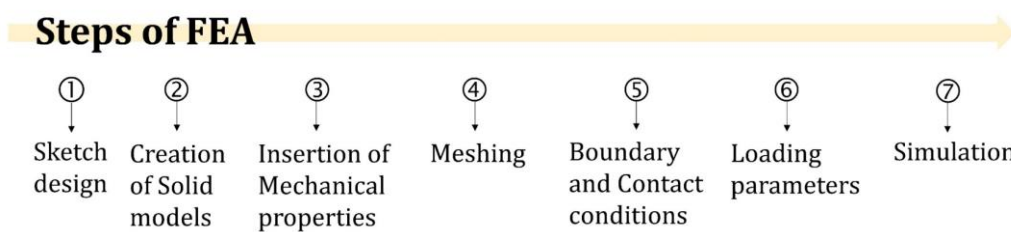


Figure 1. Step by step of Finite Element Analysis

### 2.1.1. Sketch design

The modeling process begins with the creation of a detailed sketch, which serves as the foundational blueprint for the 3D model. In this initial phase, we define the essential dimensions and geometric features of the dental crown and the underlying tooth structure (Fig. 2). The sketching process involves utilizing various tools within Fusion 360 to accurately represent the contours and critical dimensions of the crown preparation, ensuring that the model reflects the intended design specifications. Crown, PDL, cancellous bone and cortical bone were standardized (Fig. 2A). The tooth structure and cement layer were modified according to each preparation design (Fig. 2B). An offset of the tooth sketch was performed through the entire surface to create a 100 micron of cement layer, consistent with the recommended guidelines for ceramic restorations (Fig. 2C).

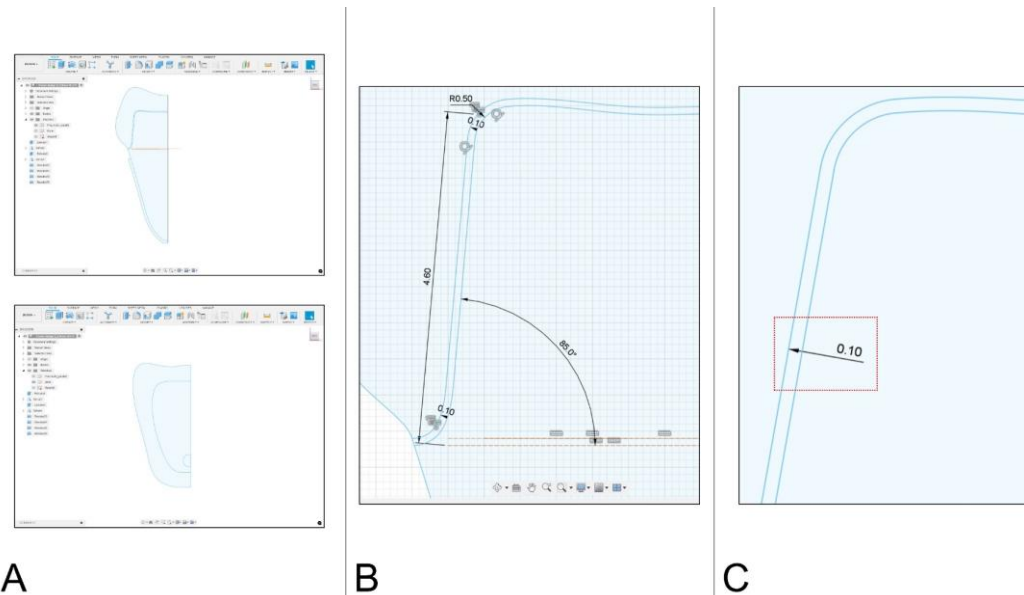


Figure 2. Sketch design of Finite Element Analysis. A. Sketch of crown, tooth structure, cement layer, periodontal ligament (PDL), cancellous bone, and cortical bone. Edges were rounded and margin was extended to minimize mesh erroring in further simulation. TOC angulation was applied regarding to each total occlusal convergence (TOC). B. Amplified visualization of cement layer, an offset of 0.1mm (100microns) was performed from the prepared tooth.

The sketch design of margin design, crown height, and TOC are shown in Figure 3. Chamfer finish line was created with a 0.5mm diameter from the margin edge (Fig. 3A). Deep chamfer finish line was created with a 1mm diameter from the margin edge (Fig. 3B). The vertical finish line (Fig. 3C) was specifically intended to simulate a clinical scenario that closely resembles typical crown preparations. The sketch of crown height was assessed from 3mm (Fig. 3D), 4.5mm (Fig. 3E), and 6mm (Fig. 3F). Furthermore, the taper degree of an axial wall was created to obtain a TOC of 10° (Fig. 3G), 20° (Fig. 3H), and 30° (Fig. 3I). It is important to note that while a vertical finish line can provide a precise

representation of the intended design, the presence of sharp edges can lead to mesh errors during the simulation process.

These errors can manifest as irregularities in the mesh, which may compromise the accuracy of the stress distribution results obtained from the FEA. To mitigate these issues, the sharp areas of the vertical finish line were rounded to create a more gradual transition between surfaces. This modification not only facilitates a smoother mesh generation but also enhances the overall quality of the finite element model. By ensuring that the mesh is well-formed and free of distortions, we can achieve more reliable and accurate simulation outcomes.

The modification of the sharped edges was realized in all sketch design. In the context of this study, the design constraints allowed for the modeling of only a single axial wall. Consequently, the angulation of this wall was determined by employing half of the total occlusal convergence (TOC) angle. The margin parallelism of 1mm was created using TOC of 20 and 30 degrees. Lastly, a sketch with the diameters of a round bur was created in the mesial surface of the tooth to evaluate auxiliary groove. The bur was designed as a round bur with a diameter of 1mm which is commonly used to create auxiliary grooves.

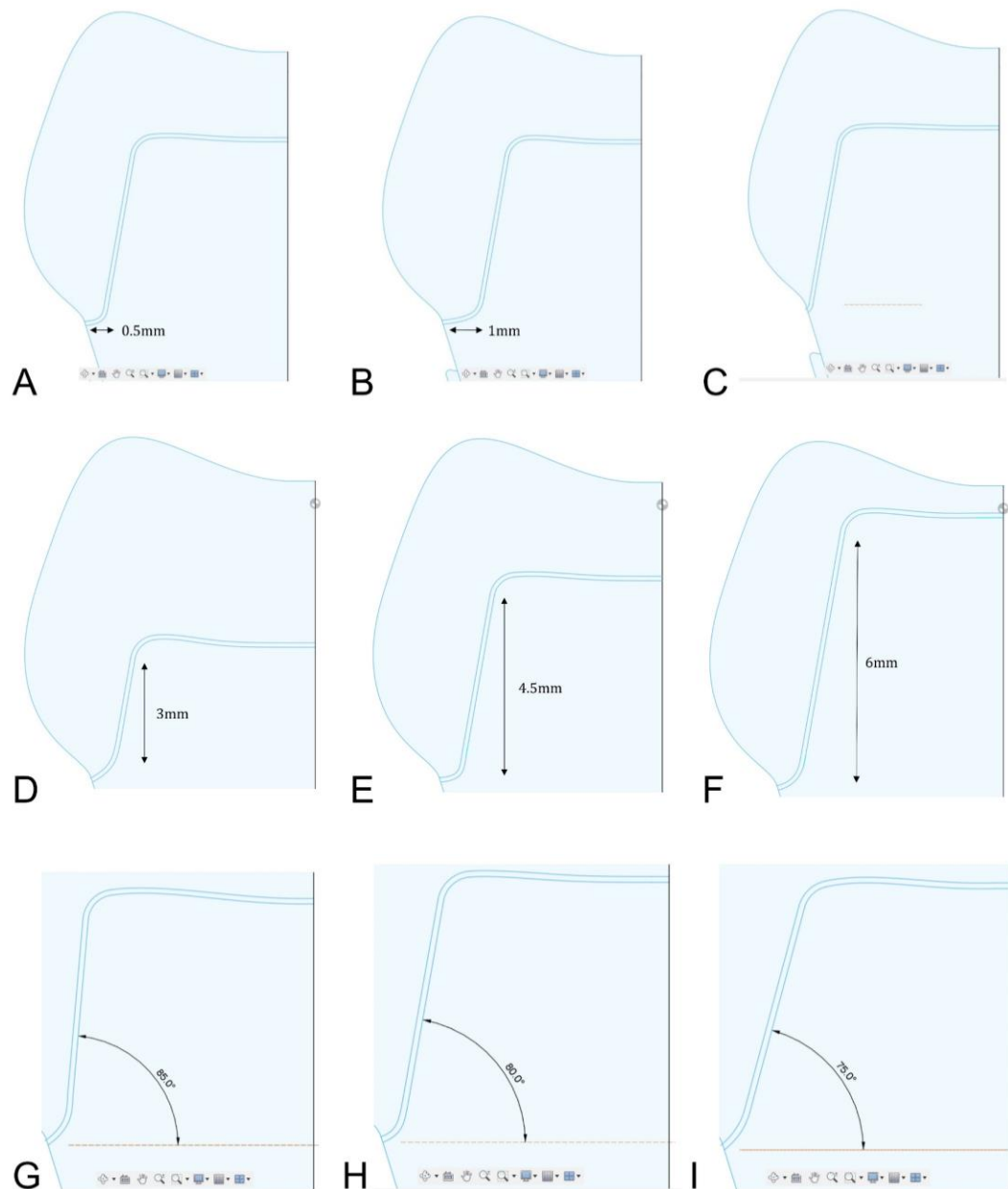


Figure 3. Sketch design of this study. A-C: Margin design: Chamfer, Deep chamfer, and Vertical. D-F: Crown height: 3mm, 4.5mm, and 6mm. G-I: TOC:  $10^\circ$ ,  $20^\circ$ , and  $30^\circ$ .

### 2.1.2. Creation of Solid models

Once the sketch is finalized, the next step involves transforming the 2D sketch into a solid body (Fig. 4). This is achieved through a process known as “extrusion”, where the sketch is extended into the third dimension to create a volumetric representation of the design. During this phase, we carefully specify the height and thickness of the crown, as well as any additional features such as margins or internal geometry.

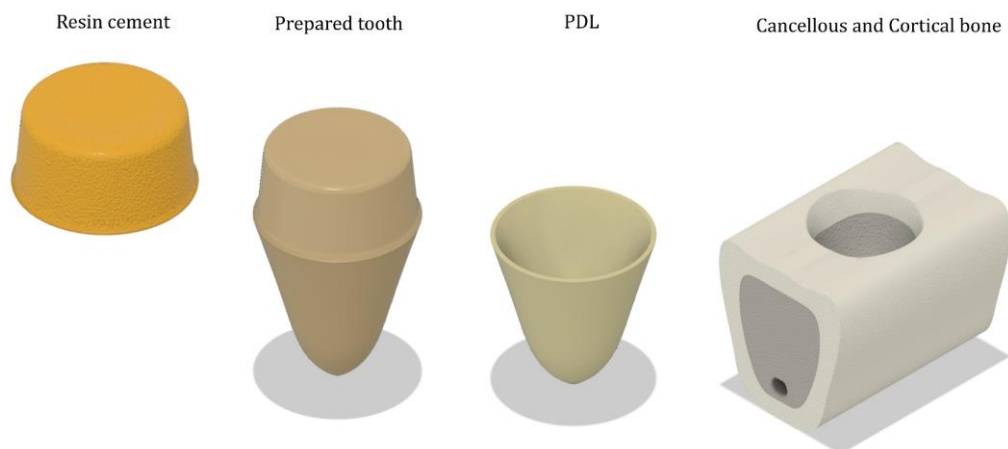


Figure 4. Solid bodies of resin cement layer, tooth structure, PDL, cancellous bone and cortical bone.

To enhance the accuracy of the model, we also incorporate relevant anatomical details, such as the curvature of the tooth and the specific design of the crown preparation (Fig. 5). This attention to detail is crucial, as it ensures that the model closely mimics the actual clinical scenario, allowing for more reliable simulation results.

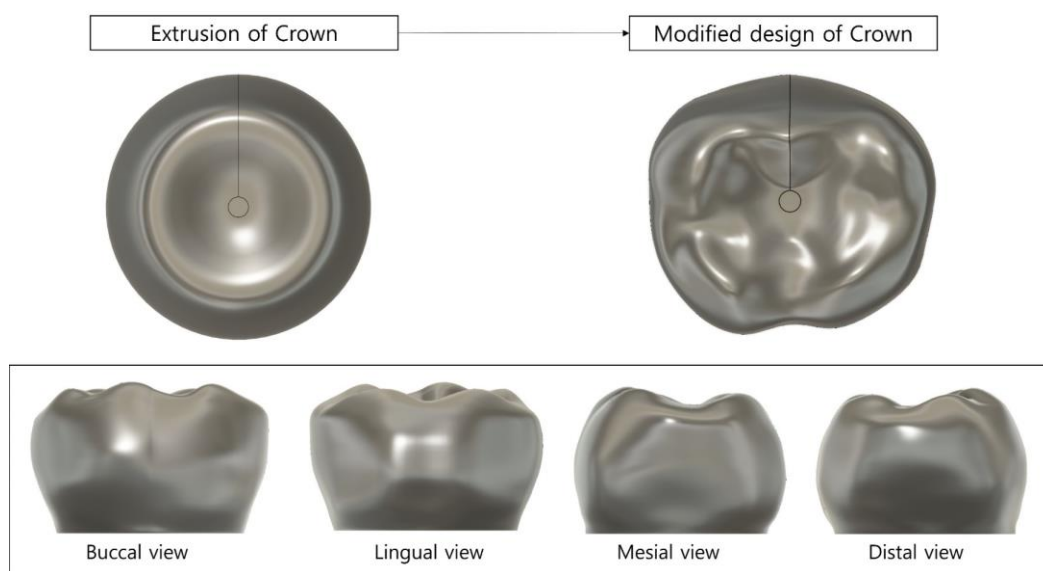


Figure 5. Anatomical modifications were made to mimic a mandibular first right molar.

Solid models were created for each design parameter (Fig. 6, 7). This process involved meticulously designing individual solid models that correspond to various configurations. In addition to the primary crown models, solid representations of diverse TOC were developed based on each finish line design and crown height.

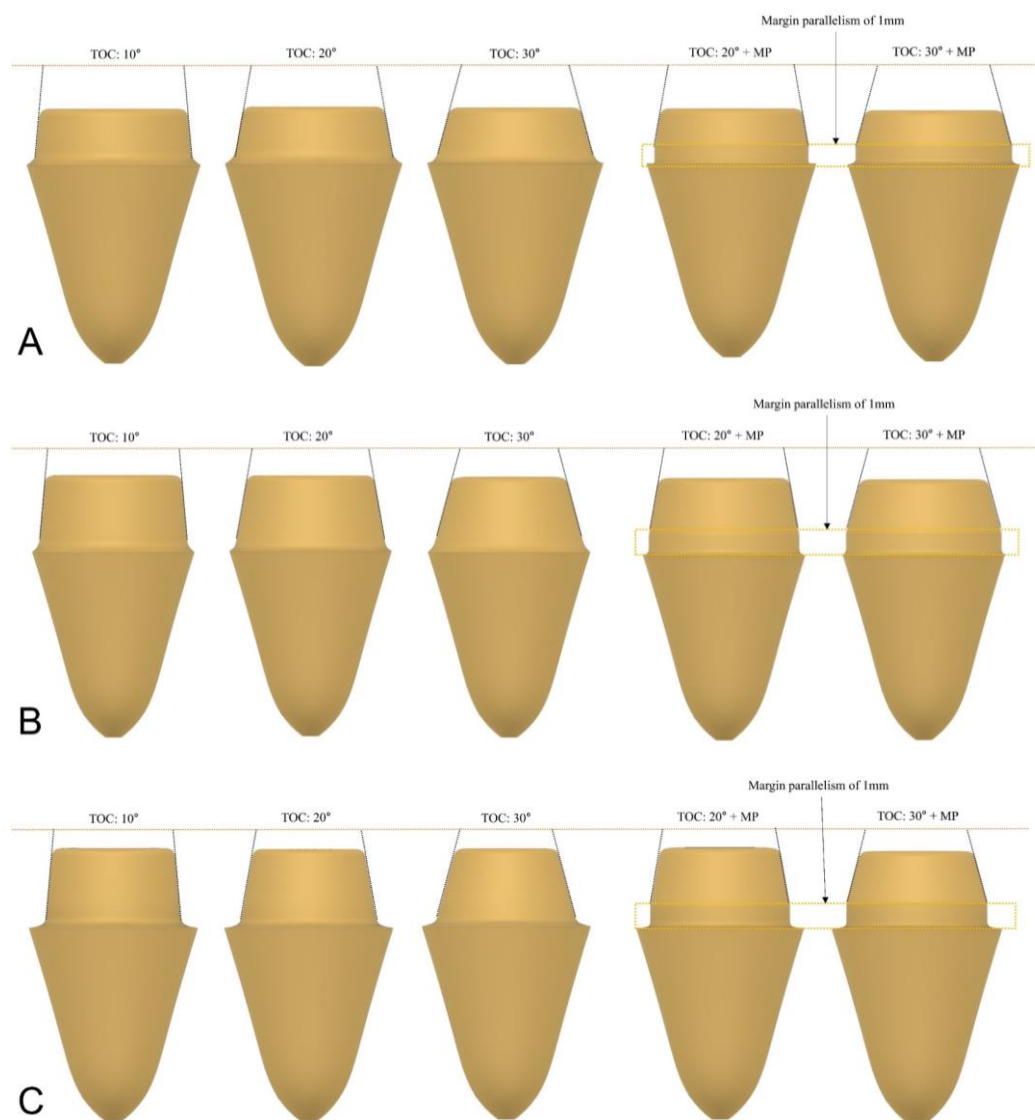


Figure 6. Three-dimensional Finite Element solid models. A. Crown height of 3mm, Chamfer finish line, TOC  $10^\circ$ ,  $20^\circ$ , and  $30^\circ$ , presence of margin parallelism of 1mm at TOC  $20^\circ$  and  $30^\circ$ . B. Crown height of 4.5mm, Chamfer finish line, TOC  $10^\circ$ ,  $20^\circ$ , and  $30^\circ$ , presence of margin parallelism of 1mm at TOC  $20^\circ$  and  $30^\circ$ . C. Crown height of 4.5mm,

Deep chamfer finish line, TOC 10°, 20°, and 30°, presence of margin parallelism of 1mm

at TOC 20° and 30°. \*TOC: Total Occlusal Convergence

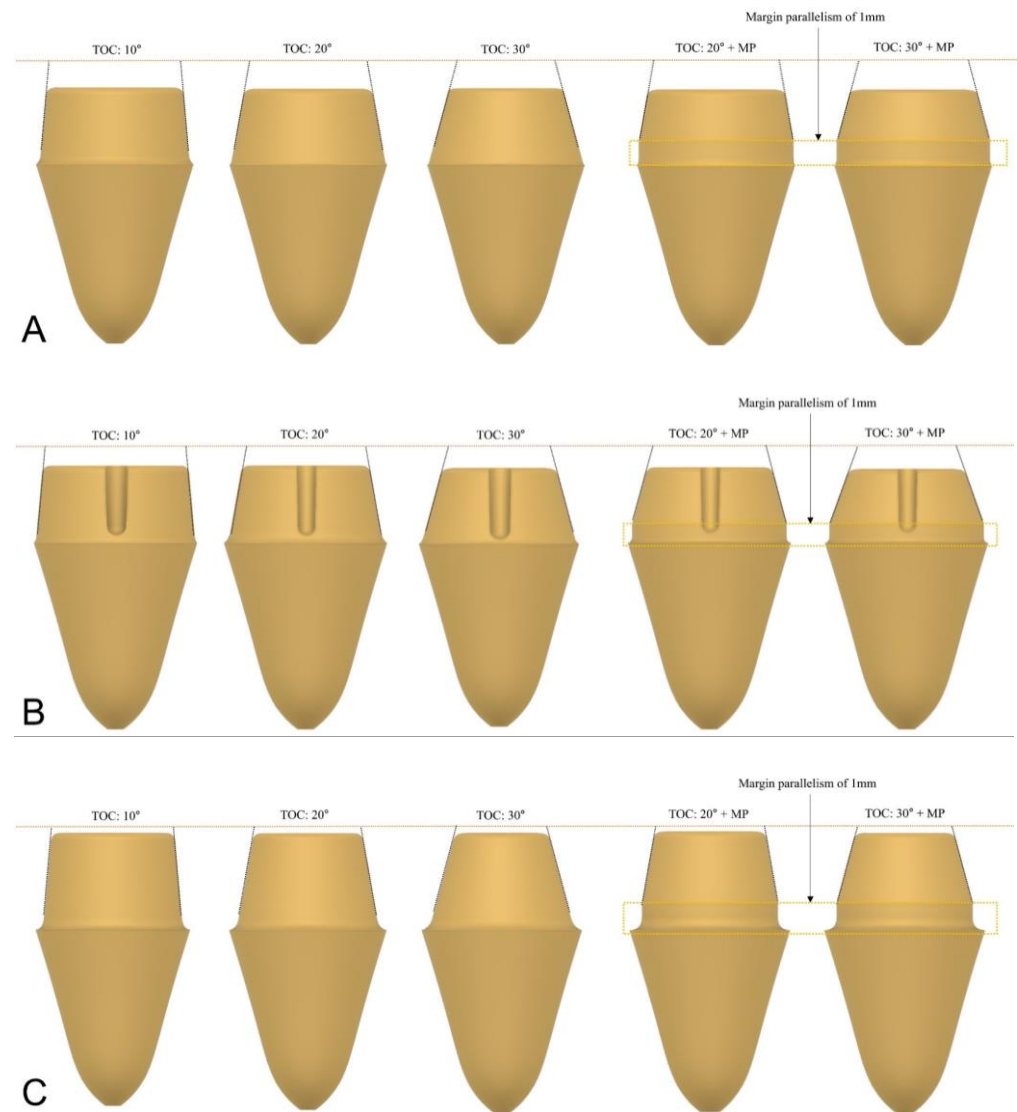


Figure 7. Three-dimensional Finite Element solid models. A. Crown height of 4.5mm, Vertical finish line, TOC 10°, 20°, and 30°, presence of margin parallelism of 1mm at TOC

20° and 30°. B. Crown height of 4.5mm, Chamfer finish line, TOC 10°, 20°, and 30°, presence of margin parallelism of 1mm at TOC 20° and 30°, presence of auxiliary mesial groove. C. Crown height of 6mm, Chamfer finish line, TOC 10°, 20°, and 30°, presence of margin parallelism of 1mm at TOC 20° and 30°. \*TOC: Total Occlusal Convergence

The auxiliary mesial groove was performed using a round bur of 1mm in diameter, which is commonly used for tooth preparation. The bur was located 1mm above the finish line according to each TOC. To ensure consistency and accuracy in the modeling process, the tooth design was standardized, utilizing a crown height of 4.5mm and a chamfer finish line. This standardization is crucial for establishing a baseline for comparison across different experimental conditions.

Once the solid bodies of the bur and tooth structure were created, both components were selected simultaneously, and the “combine” tool in the CAD software was employed. This tool allowed for the integration of the bur model with the tooth structure, facilitating the next step in the modeling process. Subsequently, the “cut” operation was performed to create the auxiliary groove within the tooth structure and cement layer. This operation effectively removed material from the tooth model, resulting in the desired groove configuration.

Additionally, the “combine” tool was utilized to modify the internal surface of the crown by filling the gap created by the bur during the preparation process. To achieve this, the tooth structure, cement layer, and crown models were selected and combined into a single entity. Once the components were combined, the “cut” operation was performed to refine the internal surfaces of the crown. This operation effectively removes any excess material and creates a precise fit between the crown and the underlying tooth structure, as well as the cement layer. Figure 8 illustrates the presence of a mesial groove in the crown, prepared tooth, and cement layer.

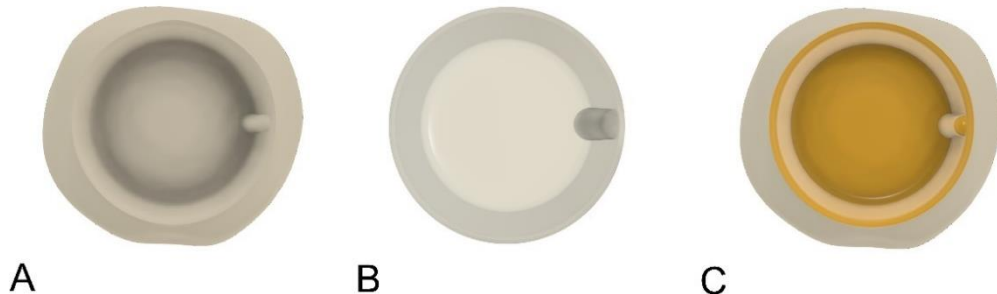


Figure 8. Three-dimensional Finite Element solid model of Auxiliary Mesial Groove. A. Internal surface of crown. B. Occlusal view of tooth structure. C. Internal surface of cement layer.

### 2.1.3. Material properties

After the solid body is created, the model was refined by applying material properties and defining boundary conditions that will be used in the FEA. This includes specifying the mechanical properties of the materials involved, such as Young's modulus and Poisson's ratio, as well as setting up the loading conditions that the crown will experience during the analysis. The mechanical properties of the solid models were selected from previous studies (Maghami et al. 2018, Luo et al. 2022) to reflect realistic clinical conditions and are summarized in Table 2.

Table 2. Mechanical properties of materials used in finite element analysis

Material	Elastic modulus (GPa)	Poisson's ratio
Monolithic Zirconia	205	0.19
Resin cement	5	0.35
Tooth structure	18.7	0.31
PDL	0.003	0.45
Cortical bone	13.7	0.30
Cancellous bone	1.37	0.25

### 2.1.4. Meshing

After the input of each material property, the next critical step in the FEA process is the creation of the mesh. The mesh was generated using tetrahedral elements, which are particularly effective for modeling complex geometries (Fig. 9). Tetrahedral meshing allows for greater flexibility in capturing the diverse shapes and contours of the models, ensuring that the finite elements conform closely to the geometry of the solid bodies. The specified mesh settings utilized in this study are detailed in Table 3.

Table 3. Mesh setting of finite elements used in this study.

Model-based size	5%
Element order	Parabolic
Created Curved Mesh Elements	Applied
Max. Turn Angle on Curves (Deg.)	60
Max. Adjacent Mesh Size Ratio	1.5
Max. Aspect Ratio	8
Minimum Element Size (% of average size)	20

A well-defined mesh is crucial, as it directly influences the quality of the simulation results. A finer mesh can provide more accurate stress distribution data, while a coarser mesh may lead to less reliable outcomes. However, it is important to mention that extensive mesh data could lead to errors of the simulation. Therefore, in this study the mesh for the cement layer was set to a finer resolution of 0.080 mm while the other components were set at 1.5mm. This refinement was implemented to obtain more accurate and precise results, as the cement layer plays a vital role in the overall mechanical performance of the crown as the weakest area among the components.



Figure 9. The tetrahedral mesh of finite elements. A. Overall view of mesh. B. The cement layer has a finer mesh size than other components. C. Amplified view of mesh form.

### 2.1.5. Boundary and Contact conditions

The structural constraints were applied to the cancellous bone and cortical bone (Fig. 10). These constraints are essential for accurately simulating the mechanical behavior of the crown and its interaction with the surrounding tooth structure. The contact conditions between the various components of the model were set to a precision of 50 microns. A contact precision of 50 microns ensures that the interface between these components is accurately represented, which is vital for understanding how forces are transmitted through the assembly during loading.

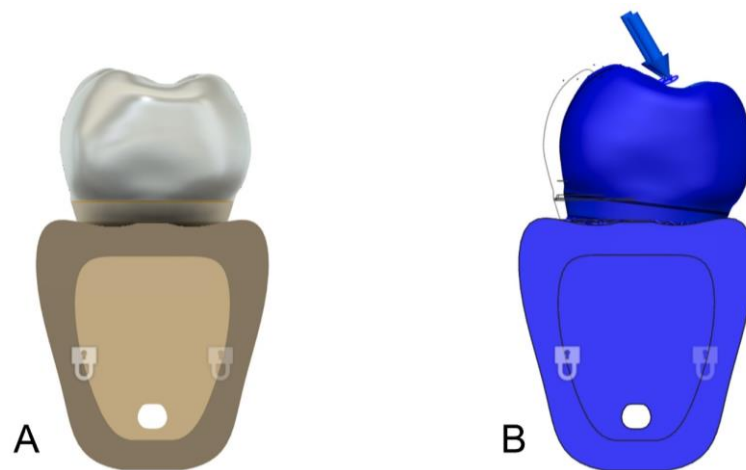


Figure 10. Structural constraints fixed at cancellous bone and cortical bone. A. Model view of constraints. B. Constraints remain fixed at loading force application.

Furthermore, the contact type was designated as ‘Bonded’ for all components. This designation indicates that the interfaces between the crown, cement layer, and tooth structure are assumed to be perfectly adhered, meaning that there is no relative movement between them under load. This assumption is particularly relevant in clinical scenarios where the cement layer effectively bonds the crown to the tooth, providing stability and support during functional use.

### 2.1.6. Loading conditions

The analysis considered multiple loading directions at the occlusal surface to replicate clinical scenarios and were divided into vertical and oblique loading directions. Furthermore, each loading direction was further divided into three distinct groups, as detailed in Fig. 11. The loading force was standardized at 200N for each loading case.

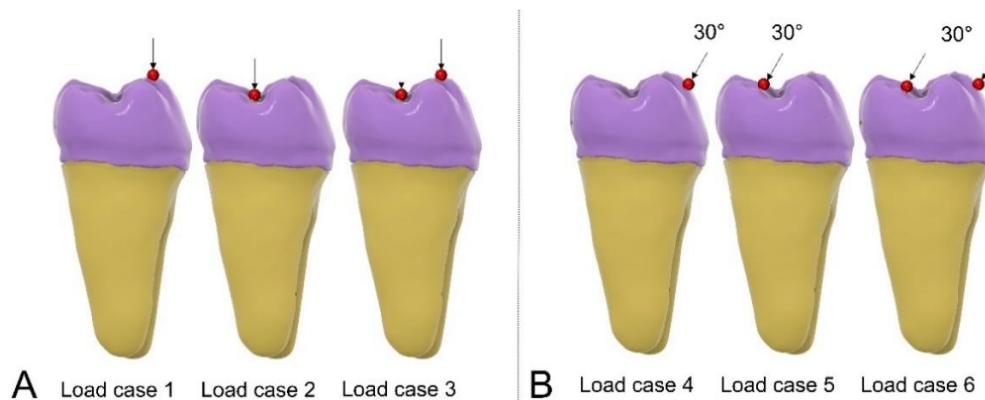


Figure 11. Loading parameters used in this study for Finite Element Analysis. 200N of force was applied. A. Vertical loading at occlusal surface. Load case 1: buccal cusps. Load case 2: central fossa. Load case 3: buccal cusps and central fossa. B. Oblique loading at

occlusal surface (Angulation of 30 degrees). Load case 1: Slightly below buccal cusps. Load case 2: Slightly below lingual cusps. Load case 3: slightly below buccal and lingual cusps.

Reference points were included in the occlusal surface of the crown to direct the loading forces in the same position for each simulation (Fig. 12). The points were located regarding the loading direction. For the vertical loading cases, three points were created at each buccal cusps and three points at central fossa (mesial, central, and distal) (Fig. 12A). For the oblique loading cases, three points were created slightly below each buccal cusps buccally and two points slightly below the lingual cusps buccally (Fig. 12B). Reference points facilitate the replication of studies, allowing other researchers to validate findings, and thereby, reducing potential human error.

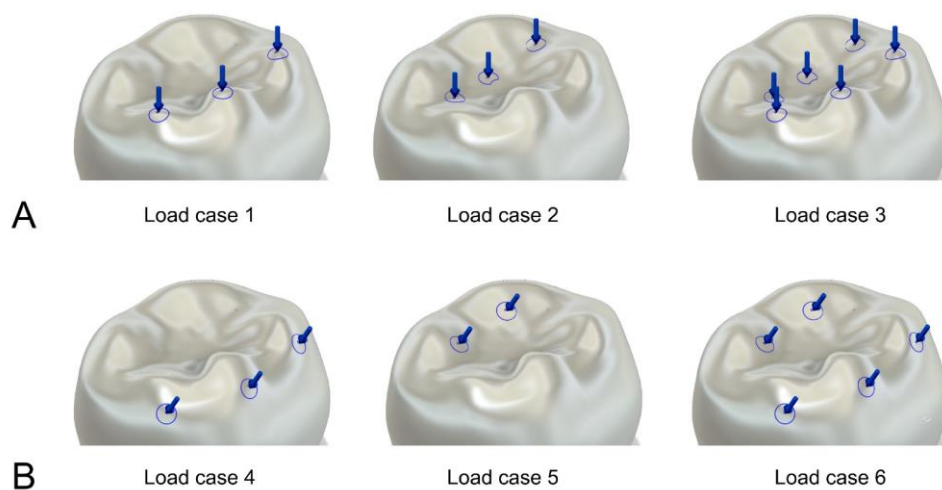


Figure 12. Reference points in the occlusal surface of the crown. A. Vertical loading cases. B. Oblique loading cases.

### 2.1.7. Simulation

This simulation yields a comprehensive array of results, including stress distribution, displacement, reaction forces, strain, contact pressure, and contact forces for each loading scenario analyzed. The stress distribution illustrates how internal stresses are distributed throughout the crown and surrounding structures, highlighting areas that may be prone to failure under load. Additionally, the simulation provides information on the quantity of nodes and elements used in the model. A higher number of nodes and elements typically indicates a more refined mesh, leading to more precise results, while also requiring greater computational resources. The results of this FEA simulation revealed a mean value of 1,104,220 nodes and 665,098 elements.

**Node count:** the total number of nodes in a finite element model represents the discrete points at which the equations of motion are solved. A mean value of over 1 million nodes indicates a highly refined mesh, which allows for a more accurate representation of the geometry and material properties of the system being analyzed. This high node count facilitates the capture of intricate details and variations in stress and strain distributions throughout the model.

**Element count:** similarly, the number of elements, which in this case is 665,098, reflects the subdivision of the model into smaller, manageable parts for analysis. A higher element count generally correlates with improved accuracy in the simulation results, as it enables the model to better approximate the physical behavior of the material under various loading conditions. Each element contributed to the overall response of the structure, and a greater number of elements allows for a more nuanced understanding of how forces are transmitted through the material.

## 2.2. In-vitro study specimen design

Following the FEA simulations, select groups were chosen for an in-vitro study to validate and compare the simulation results (Fig. 13). The aim of this in-vitro study was to evaluate the effect of different preparation designs on the cement layer, with the goal of assessing the mechanical behavior of dental crowns. Utilizing a universal testing machine, both pull-out test and occlusal loading tests were conducted to simulate the forces

experienced by crowns in clinical settings, which are described further. A non-eugenol temporary cement (TempBond, Kerr, Orange, California) was employed to facilitate easier separation of the crown from the tooth structure, allowing for a more precise analysis of the cement layer's role in crown retention and stability.

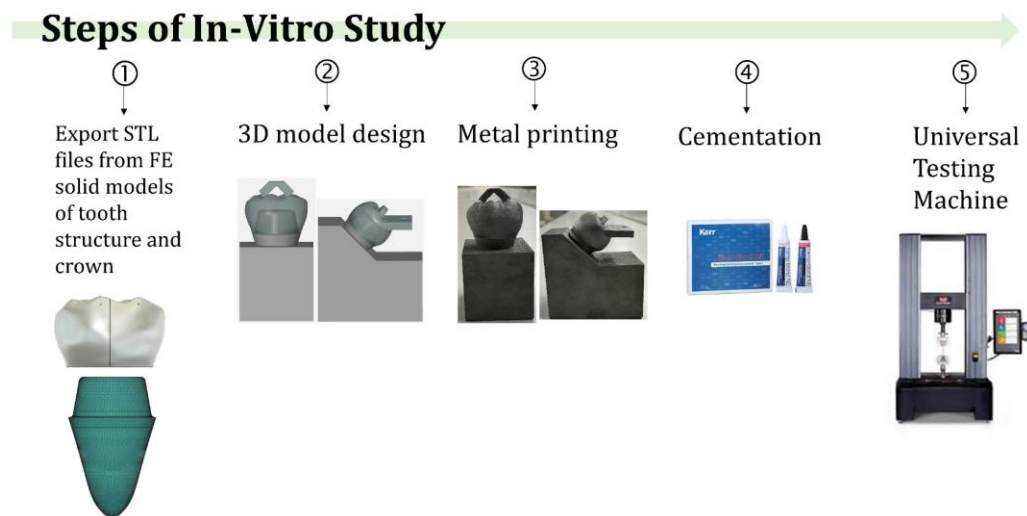


Figure 13. Description of In-vitro study.

Four studies, comprising a total of thirteen specific groups, were selected for this analysis, with detailed information provided in Table 1. Two types of evaluations were conducted: (1) a pull-out test and (2) a combined occlusal loading and pull-out test, both using a universal testing machine (UTM, Instron, Norwood, USA). The tooth preparation designs, and corresponding crowns were exported from the FEA software as stereolithography (STL) files. Additional design modifications were made to adjust the specimens for compatibility with the UTM. These modifications were carried out using CAD design software (Meshmixer, Autodesk). Each model was designed separately based on the preparation design and the type of evaluation (Fig. 14).

For the pull-out test group, a ring was added to the occlusal surface of the crown (Fig.

14A). For the occlusal loading + pull-out test group, the model was designed to accommodate both tests, where the pressure was applied through a plane created on the occlusal surface of the crown and the ring above the plane to apply the pull-out test. To ensure consistency, a hollow sphere was positioned in the center of this plane to replicate the occlusal loading force at the same point for each specimen (Fig. 14B). A total of 52 specimens were fabricated using metal 3D printing, with 26 specimens allocated to the pull-out test (crown + base) and the remaining 26 to the combined occlusal loading and pull-out test (crown + base).

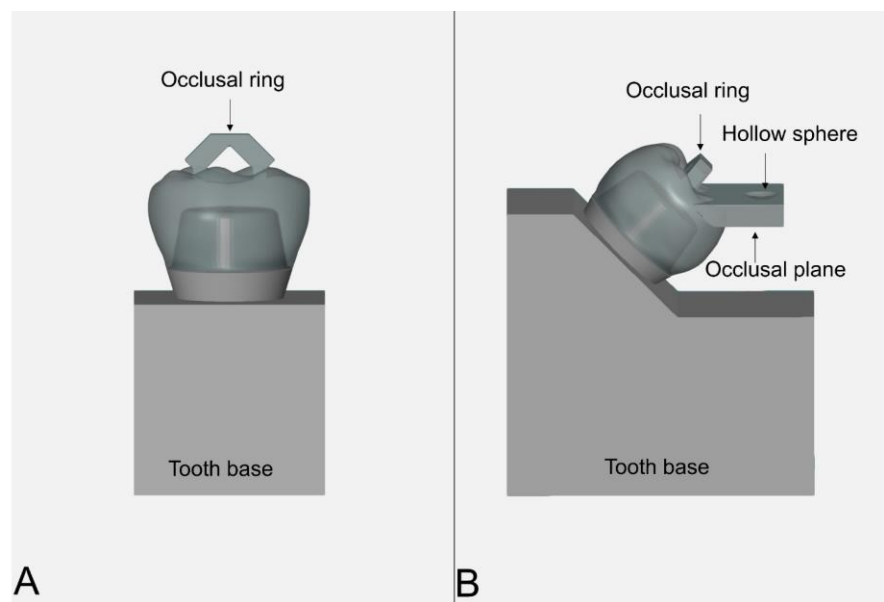


Figure 14. Modifications of each crown and preparation design for the in-vitro study. A. Pull-out test experiment design. B. Occlusal loading + Pull-out test experiment design.

For the pull-out test, a pulling force was applied through the occlusal ring using a 0.7mm orthodontic metal wire (Fig 15A). The test automatically concluded when the crown was completely separated from the base. For the occlusal loading + pull-out test, the test was halted when a significant decrease in loading force was detected (Fig. 15B). Following the occlusal loading test, the base was rotated so that it was parallel to the occlusal ring (Fig. 15C), allowing for a vertical pulling force to be applied in the subsequent test. To accomplish this, dental floss was used as these specimens required only minimal force to

achieve decementation of the crowns.

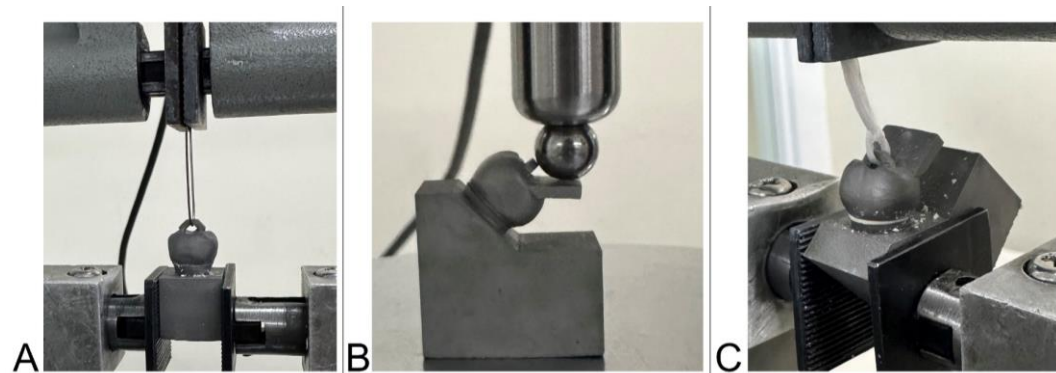


Figure 15. In-vitro study conducted using a Universal Testing Machine (UTM, Instron). A. pull-out test setup utilizing a 0.7 mm orthodontic wire to apply force. B. (a) Initial occlusal loading test performed using a plane incorporated on the occlusal surface of the crown. (b) Subsequent pull-out test conducted with dental floss to facilitate separation.

### 2.3. Statistical analysis

Statistical analysis was conducted to evaluate the significance of differences between the experimental groups regarding to the stability. Post hoc comparisons were performed using the Tukey test to identify specific differences between preparation designs and stability of crown. A significant level of  $p<0.05$  was established for all statistical tests to ensure robust and reliable results.

## 3. Results

### 3.1. Finite Element Analysis Overall Results

The overall von Mises stress values obtained from the simulations were first exported to a CSV file for further analysis in Excel. The focus was on identifying the top 50 highest stress values, which were then isolated for detailed examination. An average of these top values was calculated, allowing us to measure the peak performance while minimizing the influence of potential outliers that could distort the interpretation of the maximum data point. This approach provides a more stable and reliable assessment of the material's or structure's high-end performance.

#### 3.1.1. Crown height (3mm, 4.5mm, and 6mm)

Overall stress values of Crown heights are shown in Table 4. For crown height of 3mm, the highest values were observed in Load case 5 at a  $20^\circ + MP$  reaching 3415 MPa, and at a  $30^\circ + MP$ , peaking at 4136 MPa. Conversely, the lowest stress values were recorded in Load case 3, with a maximum of 837 MPa at a  $30^\circ + MP$ .

For crown height 4.5mm, stress values ranged from 483 MPa (Load case 3 at  $30^\circ + MP$ ) to 2894 MPa (Load case 2 at  $30^\circ MP$ ). The highest stress values were observed for Load case 2 and 4, while Load case 3 had the lowest stress. Stress tended to increase TOC with  $20^\circ$  and  $30^\circ$  when MP was applied. Crown height 6mm stress values ranged from 623 MPa (Load case 3 at  $30^\circ + MP$ ) to 3617 MPa (Load case 4 at  $30^\circ + MP$ ) to 3617 MPa (Load case 4 at  $30^\circ$ ). TOC of  $30^\circ$  without MP consistently produced the highest stress, especially for Load case 4, while Load case 3 showed the lowest stress values.

Table 4. Von mises stress values (MPa) of study group 'Crown height'

<b>CROWN HEIGHT</b>						
	Load case	10°	20°	20°+MP	30°	30°+MP
<b>3mm</b>	<b>1</b>	855	731	1286	843	1665
	<b>2</b>	1157	978	886	1335	1058
	<b>3</b>	616	518	672	699	837
	<b>4</b>	2018	2817	1963	2546	2366
	<b>5</b>	2175	2086	3415	1427	4136
	<b>6</b>	1342	1796	1614	1521	1864
<b>4.5mm</b>	<b>Load case</b>	<b>10°</b>	<b>20°</b>	<b>20°+MP</b>	<b>30°</b>	<b>30°+MP</b>
	<b>1</b>	785	757	1110	785	812
	<b>2</b>	1087	904	677	813	2894
	<b>3</b>	568	507	566	471	1450
	<b>4</b>	2653	2763	2902	2201	1734
	<b>5</b>	2575	2311	2690	2385	1315
	<b>6</b>	1766	1740	1906	1465	1063
<b>6mm</b>	<b>Load case</b>	<b>10°</b>	<b>20°</b>	<b>20°+MP</b>	<b>30°</b>	<b>30°+MP</b>
	<b>1</b>	1142	1226	1095	1118	853
	<b>2</b>	580	907	1070	915	1135
	<b>3</b>	576	631	692	621	623
	<b>4</b>	3145	2973	2468	3617	2367
	<b>5</b>	2767	2416	2271	3027	2031
	<b>6</b>	2092	1811	1616	2266	1528

\*The stress value was calculated as the average of the top 1 to 50 ranked values

\*MP: 1mm of Margin parallelism

However, it is important to note that stress concentrations in oblique loading cases vary with different crown heights. As illustrated in Figure 16, crown height of 3mm shows higher stress primarily concentrated at the occlusal surface. Likely crown height of 4.5mm shows high-stress areas at the occlusal surface, the stress distribution is more evenly spread across the crown compared to the 3mm crown height. Conversely, at a crown height of 6 mm, there is a notable decrease in stress concentration, indicating that a greater crown height may help to distribute the stress more evenly and reduce localized stress peaks. This suggests that increasing the crown height can distribute the stress concentration to the crown.

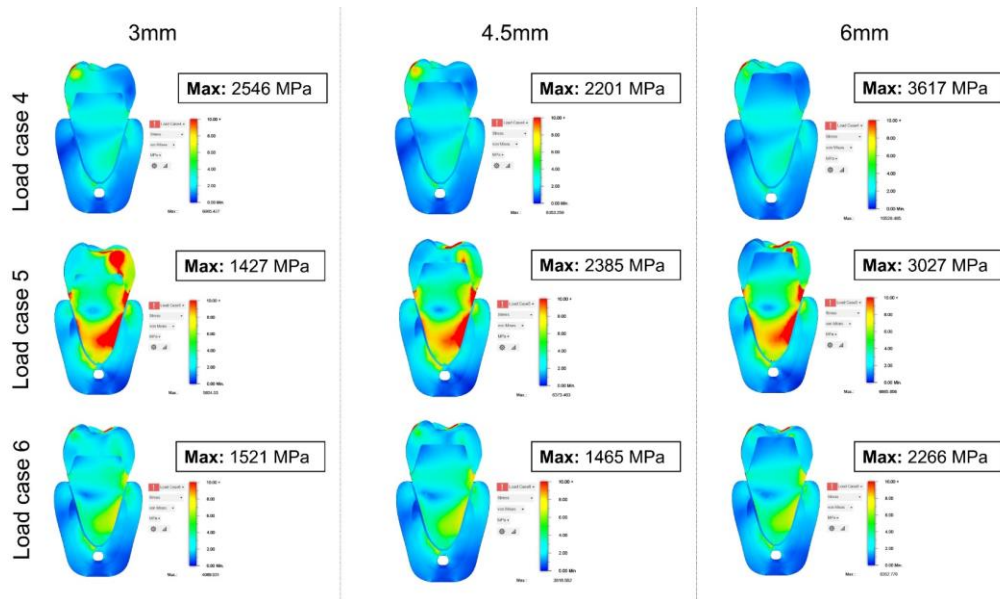


Figure 16. Bucco-lingual sectional view of Finite Element Analysis of load cases 4, 5, and 6 from Crown height group (Finish line: Chamfer / TOC: 30°)

### 3.1.2. Finish line (Chamfer, Deep chamfer, and Vertical)

Overall stress values of the study group finish line are shown in Table 5. In these results, different finish line designs (Chamfer, deep chamfer, vertical) were evaluated.

Chamfer finish line stress values ranged from 471 MPa (Load case 3 at 30°MP). Load case 4 consistently demonstrated the highest stress values, particularly at 30° TOC, while load case 3 exhibited the lowest stress values across all TOC. Deep chamfer finish line stress values varied from 465 MPa (Load case 3 at 10°) to 4126 MPa (Load case 4 at 30°MP). Load case 4 generated the highest stress at all TOC, especially at 30°MP. Load case 3 consistently showed the lowest stress values. Stress values increase with higher TOC, especially with the addition of MP. Vertical finish line stress values ranged from 545 MPa (Load cases 3 at 30°) to 3867 MPa (Load case 5 at 10°). The vertical finish line demonstrated the highest stress values in Load case 5, particularly at 10° TOC. Stress was generally higher at 10° and 20° TOC but decreased with the presence of MP at 30° TOC.

Table 5. Von mises stress values (MPa) of study group ‘Finish line’

<b>FINISH LINE</b>					
	Load case	10°	20°	20°+MP	30°
<b>Chamfer</b>	<b>1</b>	785	757	1110	785
	<b>2</b>	1087	904	677	813
	<b>3</b>	568	507	566	471
	<b>4</b>	2653	2763	2902	2201
	<b>5</b>	2575	2311	2690	2385
	<b>6</b>	1766	1740	1906	1465
<b>Deep chamfer</b>	<b>Load case</b>	<b>10°</b>	<b>20°</b>	<b>20°+MP</b>	<b>30°</b>
	<b>1</b>	842	1206	957	1151
	<b>2</b>	716	756	984	809
	<b>3</b>	465	624	558	636
	<b>4</b>	2696	2793	3063	3403
	<b>5</b>	2198	2992	2563	2924
<b>Vertical</b>	<b>Load case</b>	<b>10°</b>	<b>20°</b>	<b>20°+MP</b>	<b>30°</b>
					<b>30°+MP</b>

<b>1</b>	1240	905	1271	755	1056
<b>2</b>	983	1241	1090	941	827
<b>3</b>	667	667	715	545	595
<b>4</b>	3756	2838	3533	2826	2602
<b>5</b>	3867	3282	3131	2034	1368
<b>6</b>	2455	1868	2220	1729	1566

\*The stress value was calculated as the average of the top 1 to 50 ranked values

\*MP: 1mm of Margin parallelism

Stress distribution within the finish line group at load cases 4,5 and 6 can be observed in Fig. 17. Finish lines chamfer and deep chamfer show moderate stress levels in Load case 4 compared to vertical finish line. Furthermore, all finish line designs show increased stress concentrations at the occlusal surface in Load cases 5 and 6.

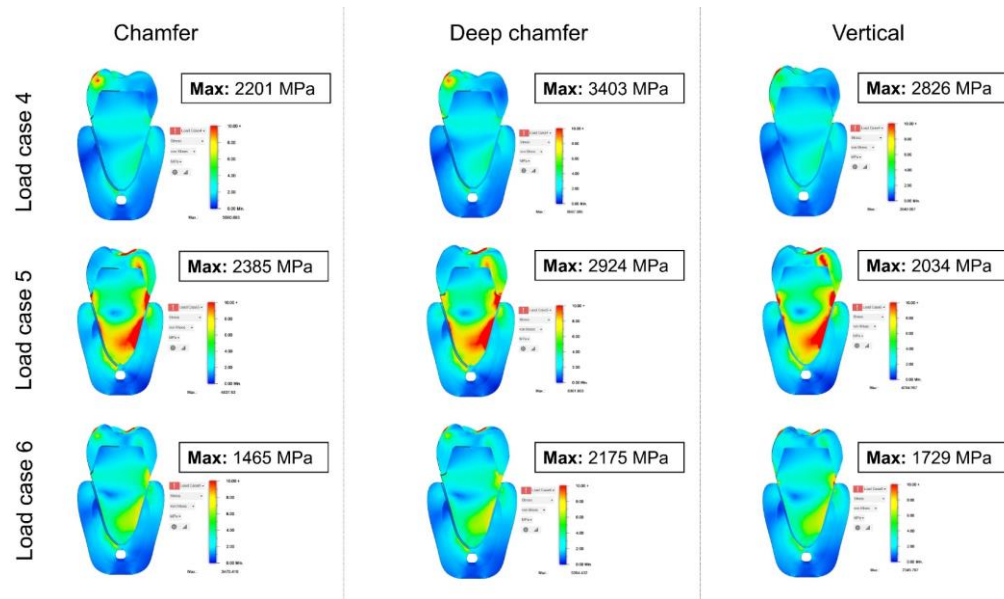


Figure 17. Bucco-lingual sectional view of Finite Element Analysis of load cases 4, 5, and 6 from Finish line group. (Crown height: 4.5mm / TOC: 30°)

### 3.1.3. Auxiliary groove (Mesial groove)

Overall stress values of the study group auxiliary mesial groove are shown in Table 6. The stress values varied from 390 MPa (Load case 3 at 30°) to 3104 MPa (Load case 5 at 30°). The auxiliary groove caused stress reduction at higher TOC (particularly 30°+MP). Load case 5 showed the highest stress without MP, while Load case 3 exhibited the lowest values consistently across all TOC. The addition of a mesial groove in the tooth preparation design plays a crucial role in stress distribution. The mesial groove effectively redistributes stress concentrations that would otherwise be localized at a single point. The mesial groove can act as a stress-relief feature.

Table 6. Von mises stress values (MPa) of study group ‘Auxiliary groove’

MESIAL GROOVE(Crown height of 4.5 mm – Finish line Chamfer)				
Load case	20°	20°+MP	30°	30°+MP
1	1044	721	675	685
2	815	586	881	627
3	550	396	475	390
4	2939	1562	3031	1235
5	2814	1621	3104	1252
6	1891	1007	2170	782

\*The stress value was calculated as the average of the top 1 to 50 ranked values

\*MP: 1mm of Margin parallelism

Figure 18 illustrates the stress distribution for the mesial groove and no groove across load cases 4,5, and 6. The mesial groove group shows more even distribution of stress, particularly in load cases 4 and 5. In contrast, the no groove group displays localized areas of high stress, particularly in load case 4, indicating potential failure points.

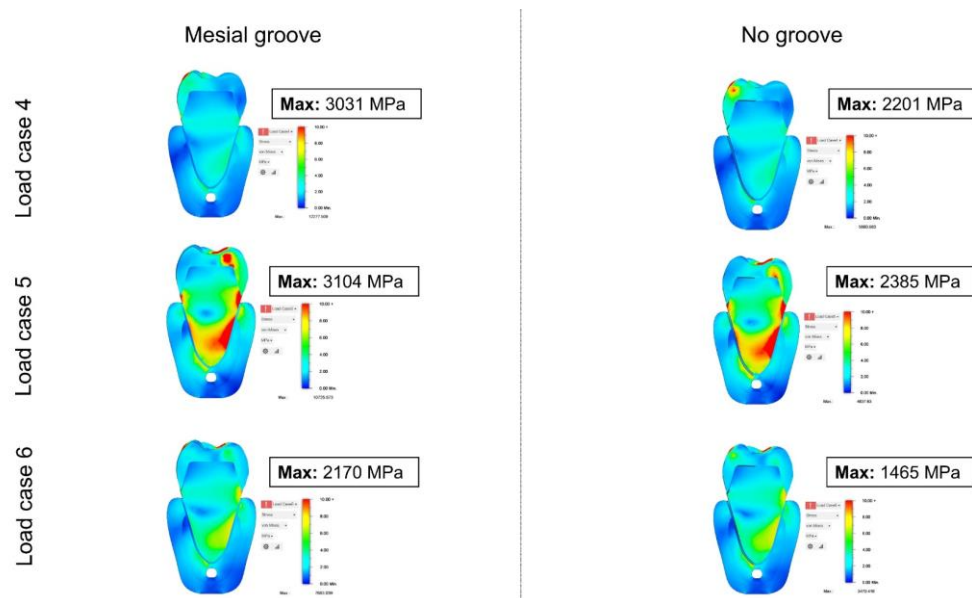


Figure 18. Bucco-lingual sectional view of Finite Element Analysis of load cases 4, 5, and 6 between Auxiliary mesial groove and No groove. (Crown height: 4.5mm / TOC: 30°/ Finish line: Chamfer)

The stress values of crown in load case 5 are summarized in Table 7. The highest stress recorded was 4136 MPa for the crown height of 3mm with chamfer finish line at a 30°+MP,

indicating significant impact of both TOC and loading conditions on stress values. in contrast, the lowest stress value of 1252 MPa was observed in the crown height of 4.5mm with auxiliary mesial groove (GR) at a 30°+MP.

The crown height of 4.5mm with vertical finish line consistently exhibited high stress values, peaking at 3867 MPa at 10° TOC, while the crown height of 4.5mm with deep chamfer finish line showed a notable increase in stress under 20° and 30° TOC, suggesting that deeper chamfer and vertical finish lines, at increased TOC may lead to higher stress values.

Table 7. Comprehensive FEA stress of crown based on multiple design factors in Load case 5

<b>STUDY</b>	<b>Total Occlusal Convergence</b>				
	10°	20°	20°+MP	30°	30°+MP
<b>3mm/Chamfer</b>	2175	2086	3415	1427	4136
<b>4.5mm/Chamfer</b>	2575	2311	2690	2385	1315
<b>4.5mm/Deep chamfer</b>	2198	2992	2563	2924	2717
<b>4.5mm/Vertical</b>	3867	3282	3131	2034	1368
<b>4.5mm/Chamfer/GR</b>		2814	1621	3104	1252
<b>6mm/Chamfer</b>	2767	2416	2271	3027	2031

\*Stress value (MPa) calculated as the average of the top 1 to 50 ranked values

\*MP: 1mm of Margin parallel

\*GR: Mesial groove

### 3.2. Von stress values (MPa) on the tooth structure

#### 3.2.1. Crown height (3mm, 4.5mm, and 6mm)

The von Mises stress values of tooth structure from crown height group is shown in Table 8. 3mm crown height shows the highest stress values across all conditions specifically in load case 5 with a peak value of 31MPa at 20°+MP. Stress value tends to increase with the addition of MP compared to other crown heights. 4.5mm crown height shows the highest stress with a peak of 22MPa at 30°+MP.

Table 8. FEA maximum stress values (MPa) of the tooth structure of Crown height group.

CROWN HEIGHT						
	Load case	10°	20°	20°+MP	30°	30°+MP
3mm	<b>1</b>	10	9	20	9	18
	<b>2</b>	6	5	11	5	9
	<b>3</b>	6	5	12	5	11
	<b>4</b>	8	8	14	7	13
	<b>5</b>	17	17	31	17	28
	<b>6</b>	10	10	18	9	16
4.5mm	<b>Load case</b>	<b>10°</b>	<b>20°</b>	<b>20°+MP</b>	<b>30°</b>	<b>30°+MP</b>
	<b>1</b>	9	9	13	9	13
	<b>2</b>	7	6	8	5	8
	<b>3</b>	6	5	8	5	7
	<b>4</b>	10	8	10	9	10
	<b>5</b>	21	16	17	16	22
6mm	<b>Load case</b>	<b>10°</b>	<b>20°</b>	<b>20°+MP</b>	<b>30°</b>	<b>30°+MP</b>
	<b>1</b>	9	9	9	9	9
	<b>2</b>	6	6	5	6	5
	<b>3</b>	6	6	5	5	5

<b>4</b>	9	9	8	8	7
<b>5</b>	18	20	15	17	15
<b>6</b>	13	12	10	10	10

\*Maximum stress values (MPa) - \*MP: 1mm of Margin parallelism

### 3.2.2. Finish line (Chamfer, Deep chamfer, and Vertical)

The von Mises stress values of tooth structure from finish line group is shown in Table 9. Load case 5 shows the highest stress values, with a peak of 22MPa at 30°+MP. The addition of MP generally increases stress values, particularly noticeable in Load cases 1 and 5. Deep chamfer finish line stress values are generally lower compared to the chamfer and vertical designs. Vertical finish line stress values are significantly higher compared to the chamfer and deep chamfer designs, particularly in Load case 5, which peaks at 46MPa at 20°.

Table 9. FEA maximum stress values (MPa) of the tooth structure of Finish line group.

<b>FINISH LINE</b>					
	<b>Load case</b>	<b>10°</b>	<b>20°</b>	<b>20°+MP</b>	<b>30°</b>
Chamfer	<b>1</b>	9	9	13	9
	<b>2</b>	7	6	8	5
	<b>3</b>	6	5	8	5
	<b>4</b>	10	8	10	9
	<b>5</b>	21	16	17	16
	<b>6</b>	12	10	14	11
Deep chamfer	<b>Load case</b>	<b>10°</b>	<b>20°</b>	<b>20°+MP</b>	<b>30°</b>
	<b>1</b>	8	8	8	8
	<b>2</b>	5	5	5	5
	<b>3</b>	5	5	5	5
	<b>4</b>	7	7	8	7
	<b>5</b>	14	14	15	16

	<b>6</b>	<b>9</b>	<b>9</b>	<b>9</b>	<b>10</b>	<b>11</b>
Vertical	<b>Load case</b>	<b>10°</b>	<b>20°</b>	<b>20°+MP</b>	<b>30°</b>	<b>30°+MP</b>
	<b>1</b>	11	28	12	19	12
	<b>2</b>	6	17	8	10	7
	<b>3</b>	7	16	7	11	7
	<b>4</b>	9	22	10	17	9
	<b>5</b>	20	46	24	31	20
	<b>6</b>	12	26	14	18	12

\*Maximum stress values (MPa) - \*MP: 1mm of Margin parallelism

### 3.2.3. Auxiliary groove (Mesial groove)

The von Mises stress values of tooth structure from auxiliary group is shown in Table 10. Load case 5 consistently shows the highest stress values across all TOC, with a peak of 28MPa at 30° indicating significant stress concentration. The addition of MP generally increases stress values, particularly noticeable in Load cases 4 and 5.

Table 10. FEA maximum stress values (MPa) of the tooth structure of Auxiliary groove group.

Auxiliary groove:	<b>Load case</b>	<b>20°</b>	<b>20°+MP</b>	<b>30°</b>	<b>30°+MP</b>
Mesial groove	<b>1</b>	12	12	11	13
	<b>2</b>	6	7	6	7
	<b>3</b>	7	7	6	8
	<b>4</b>	8	10	9	10
	<b>5</b>	19	23	28	22
	<b>6</b>	11	13	11	13

\*Maximum stress values (MPa) - \*MP: 1mm of Margin parallelism

### 3.3. Von stress values (MPa) on the cement layer

Furthermore, the von mises stress values of the cement layer were assessed. The cement layer serves as the interface between the crown and the tooth structure and is recognized as the most vulnerable region within the overall assembly. Analyzing the stress distribution within this interface is essential for understanding the mechanical behavior and potential failure mechanisms of the restoration.

#### 3.3.1. Crown height (3mm, 4.5mm, and 6mm)

Maximum stress values of crown heights are shown in Table 11. Crown height of 3mm exhibited the highest stress value of 16 MPa in Load case 1, while the 20° TOC achieved a peak stress of 28 MPa in Load case 5. Conversely, the TOC of 20°+MP consistently showed lower stress values, particularly 5 MPa in Load cases 2 and 3. In contrast, the crown height of 4.5m exhibits more consistent stress levels, with the highest value of 26 MPa in Load case 5 at a 30° TOC. The crown height of 6mm shows relatively lower stress values overall, with the maximum stress of 19 MPa.

The crown height of 6mm shows relatively lower stress values overall, with the maximum stress of 19 MPa in Load case 5 at a 10° TOC. Notably, the crown height of 3mm demonstrates significantly higher stress concentrations, particularly in Load case 5, compared to the other crown heights, indicating that shorter crowns may be more susceptible to stress under certain loading conditions.

Table 11. FEA maximum stress values (MPa) of the cement layer of Crown height group.

CROWN HEIGHT		Load case	10°	20°	20°+MP	30°	30°+MP
3mm	<b>1</b>	16	10	8	15	8	
	<b>2</b>	7	11	7	9	5	
	<b>3</b>	10	8	5	9	5	
	<b>4</b>	9	9	7	12	7	
	<b>5</b>	20	28	15	20	17	
	<b>6</b>	13	14	9	16	11	
4.5mm	<b>Load case</b>	<b>10°</b>	<b>20°</b>	<b>20°+MP</b>	<b>30°</b>	<b>30°+MP</b>	
	<b>1</b>	13	18	11	14	12	
	<b>2</b>	8	7	7	11	8	
	<b>3</b>	8	12	7	9	8	
	<b>4</b>	13	15	10	12	8	
	<b>5</b>	23	16	17	21	14	
6mm	<b>Load case</b>	<b>10°</b>	<b>20°</b>	<b>20°+MP</b>	<b>30°</b>	<b>30°+MP</b>	
	<b>1</b>	10	12	18	14	13	
	<b>2</b>	10	9	8	10	7	
	<b>3</b>	7	7	11	8	9	
	<b>4</b>	13	9	13	13	10	
	<b>5</b>	19	14	18	17	19	
	<b>6</b>	12	10	11	9	12	

\*Maximum stress values (MPa) - \*MP: 1mm of Margin parallelism

Figure 19 illustrates the stress distribution in crown height group under load cases 4, 5, and 6. Crown height of 3mm exhibits moderate stress level in Load case 4 and stress concentrations are notably high, particularly at the crown's edges. The stress distribution indicates critical stress concentrations especially at the margins. Crown height of 6mm

demonstrates the most favorable stress distribution, the stress levels remain stable across all load cases, indicating better resistance to stress concentrations.

Load case 5 consistently results in the highest stress values across all crown heights. Load cases 4 and 6 show lower stress levels, but the trend indicates that increasing load leads to significant stress increases, particularly in shorter crowns.

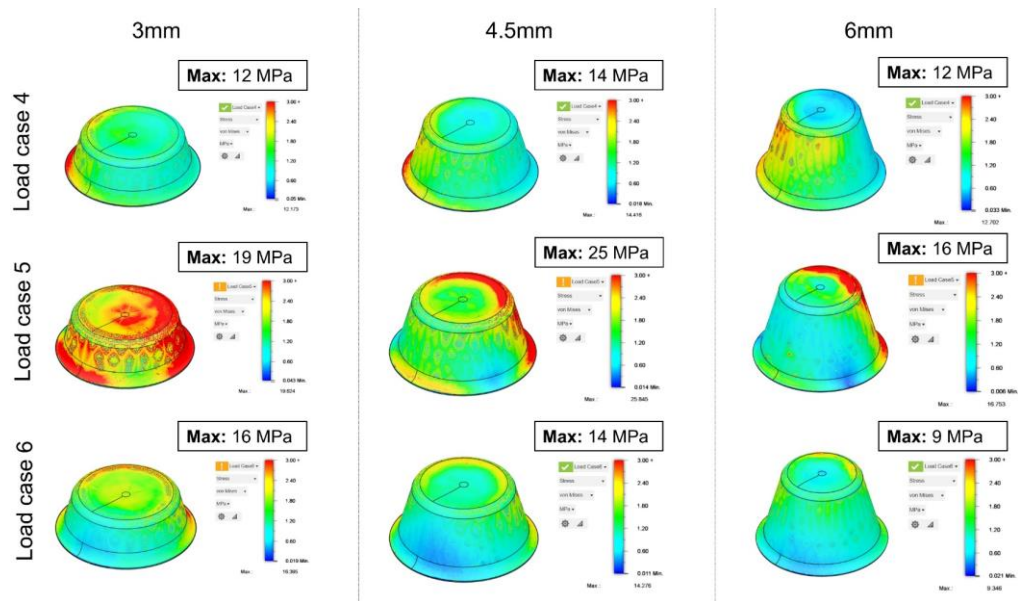


Figure 19. Cement layer view of Finite Element Analysis of load cases 4, 5, and 6 from Crown height group (Finish line: Chamfer/TOC:30°)

### 3.3.2. Finish line (Chamfer, Deep chamfer, and Vertical)

Maximum stress values of crown heights are shown in Table 12. For the chamfer design, the highest stress value occurs in Load case 5 at a 10° TOC, reaching 23 MPa, while Load case 4 shows a notable peak of 15 MPa at a 20° TOC. The deep chamfer design exhibits the highest stress of 24 MPa in Load case 5 at both 20°+MP and 30° TOC, indicating a strong performance under these conditions. In the vertical design, the

maximum stress is observed in Load case 5 at a 20° TOC, reaching 26 MPa, which is the highest value across all designs and load cases.

Table 12. FEA maximum stress values (MPa) of the cement layer of Finish line group.

<b>FINISH LINE</b>						
	<b>Load case</b>	<b>10°</b>	<b>20°</b>	<b>20°+MP</b>	<b>30°</b>	<b>30°+MP</b>
Chamfer	<b>1</b>	13	18	11	14	12
	<b>2</b>	8	7	7	11	8
	<b>3</b>	8	12	7	9	8
	<b>4</b>	13	15	10	12	8
	<b>5</b>	23	16	17	21	14
	<b>6</b>	12	10	11	12	10
Deep chamfer	<b>Load case</b>	<b>10°</b>	<b>20°</b>	<b>20°+MP</b>	<b>30°</b>	<b>30°+MP</b>
	<b>1</b>	12	12	22	15	12
	<b>2</b>	8	10	11	9	9
	<b>3</b>	9	9	14	9	8
	<b>4</b>	13	10	19	10	12
	<b>5</b>	17	21	24	24	22
Vertical	<b>Load case</b>	<b>10°</b>	<b>20°</b>	<b>20°+MP</b>	<b>30°</b>	<b>30°+MP</b>
	<b>1</b>	12	20	12	11	14
	<b>2</b>	7	10	7	10	9
	<b>3</b>	7	12	8	7	9
	<b>4</b>	9	16	10	9	10
	<b>5</b>	14	26	18	25	20
	<b>6</b>	9	15	9	14	12

\*Maximum stress values (MPa) - \*MP: 1mm of Margin parallelism

Figure 20 presents a comparative analysis of stress distribution across the finish line designs under load cases 4,5, and 6. Chamfer design shows an increase in stress in Load

case 5, particularly at the marginal area. Deep chamfer design shows an increased stress concentration in Load case 5 appearing at the margin and the internal surface. For vertical design, the stress concentration in Load case 5 rises particularly at the crown's edge.

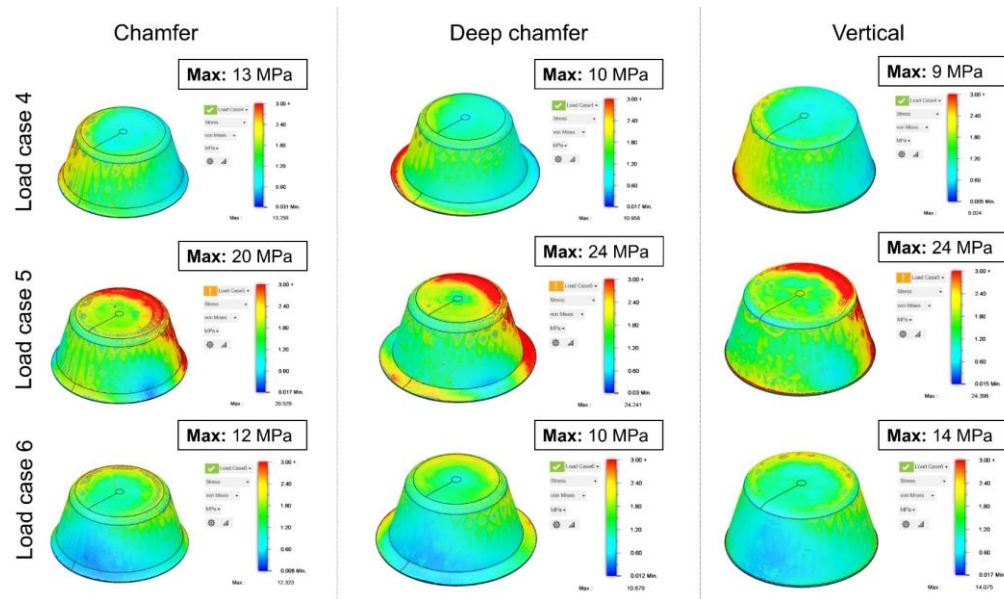


Figure 20. Cement layer view of Finite Element Analysis of load cases 4, 5, and 6 from Finish line group (Crown height:4.5mm/TOC:30°)

### 3.3.3. Auxiliary groove (Mesial groove)

Table 13 presents stress values (MPa) for auxiliary mesial groove group across the load cases and TOC. The TOC of 20°+MP exhibited the highest stress value of 14 MPa in Load case 1, while the TOC of 20° demonstrated a peak stress of 16 MPa in Load case 5, matching the TOC of 30°. The TOC of 20° consistently provided effective load distribution, particularly in Load cases 2 and 3, while the TOC of 20°+MP showed superior performance

in Load case 4 with a stress value of 12 MPa.

Table 13. Finite element analysis maximum stress values (MPa) of the cement layer of auxiliary mesial groove.

Auxiliary groove:	Load case	20°	20°+MP	30°	30°+MP
Mesial groove	<b>1</b>	12	14	11	11
	<b>2</b>	8	6	7	6
	<b>3</b>	7	8	8	7
	<b>4</b>	9	12	10	10
	<b>5</b>	16	15	16	15
	<b>6</b>	9	9	9	8

\*Maximum stress values (MPa) - \*MP: 1mm of Margin parallelism

Figure 21 illustrates the stress distribution with and without mesial groove across load cases 4, 5, and 6. Mesial groove stress concentrations remains at the groove and margin. Whereas no groove stress concentrations result in a more uniform distribution, the stress levels rise primarily at the crown's edge.

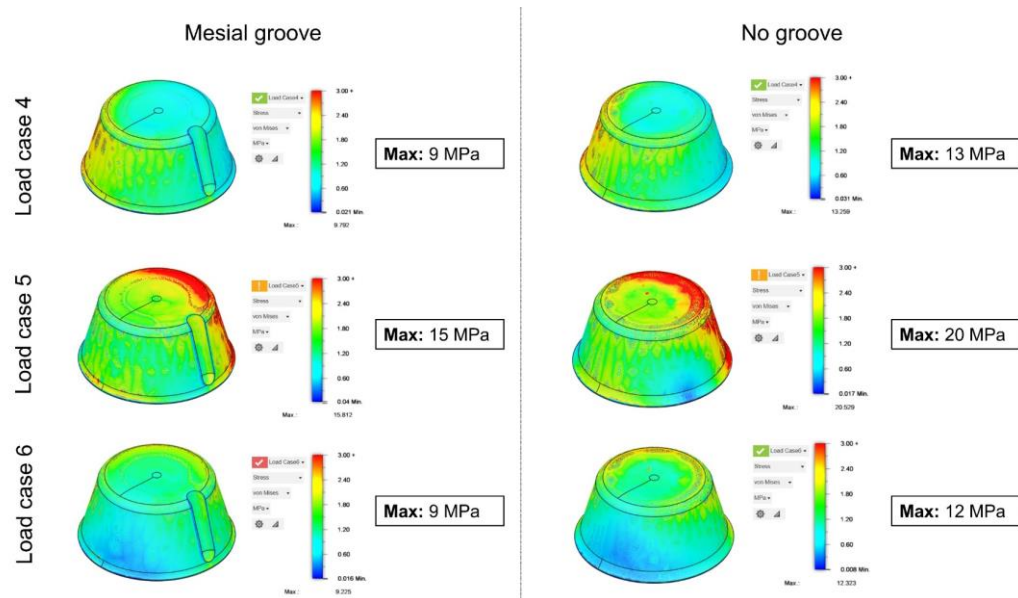


Figure 21. Finite Element Analysis results on cement layer of load cases 4, 5, and 6 from between groups ‘No groove’ and ‘Mesial groove’. (Crown height: 4.5mm/ TOC:30°)

Max stress values of cement layer in Load case 5 are summarized in Table 14. Crown height of 3mm with chamfer finish line exhibited the highest stress values at TOC of 10° and 30°, with 20 MPa and 17 MPa, respectively, while the crown height of 4.5mm with chamfer finish line showed a notable increase in stress at 30° TOC, reaching 26 MPa. The 4.5mm with deep chamfer finish line maintained relatively consistent stress values across all TOC, 4.5mm with vertical finish line also demonstrated significant stress variation, particularly at 20° TOC with 26 MPa. In contrast, the crown height of 4.5mm with mesial groove (GR) displayed lower stress values overall, with a maximum of 16 MPa. The crown height of 6mm with chamfer finish line showed moderate stress levels, with a peak of 19 MPa at both TOC of 10° and 30°.

Table 14. Comprehensive FEA stress of cement layer based on multiple design factors in Load case 5

STUDY	Total Occlusal Convergence				
	10°	20°	20°+MP	30°	30°+MP
<b>3mm/Chamfer</b>	20	28	15	20	17
<b>4.5mm/Chamfer</b>	13	18	13	26	14
<b>4.5mm/Deep chamfer</b>	17	21	24	24	22
<b>4.5mm/Vertical</b>	14	26	18	25	20
<b>4.5mm/Chamfer/GR</b>		16	15	16	15

<b>6mm/Chamfer</b>	19	14	18	17	19
--------------------	----	----	----	----	----

\*Max stress value (MPa) of cement layer

\*MP: 1mm of Margin parallel

\*GR: Mesial groove

### 3.4. In-vitro Study Results

In-vitro study was conducted to demonstrate the effect of TOC, finish line type, crown height, and auxiliary groove on the stress distribution and separation forces of the full-coverage crown at cement layer. The mean and standard deviation are shown in Table 15. The 1st evaluation consisted of evaluating the specimens under pull-out strength (N).

#### 3.4.1. Pull-out test

Table 15. Pull-out test results of In-vitro study

<b>Study</b>	<b>Groups</b>	<b>Pull out test (N)</b>
<b>TOC</b>	Group 1: 20°	198.15±69.57
	Group 2: 20°+MP	207.28±97.44
	Group 3: 30°	149.22±39.77
	Group 4: 30°+MP	162.51±50.42
<b>FINISH LINE</b>	Group 1: Chamfer	232.29±43.67
	Group 2: Deep chamfer	193.28±44.59
	Group 3: Vertical	229.41±67.31
<b>AUXILIAR GROOVE</b>	Group 1: No groove (3mm-30°)	121.25±34.23 <sup>a</sup>
	Group 2: Mesial groove (4.5mm- 30°)	170.32±52.24 <sup>b</sup>
	Group 2: Mesial groove (4.5mm-30°+MP)	178.93±42.72 <sup>b</sup>
<b>CROWN HEIGHT</b>	Group 1: 3mm	88.89±10.50 <sup>a</sup>
	Group 2: 4.5mm	198.15±69.57 <sup>b</sup>

---

Group 3: 6mm	175.07±13.45 <sup>b</sup>
--------------	---------------------------

---

\*Mean and standard deviation values (N)

\*Same superscript letters within the column show no statistical significance within the groups.

For TOC study (Fig. 22), Group 1( $20^\circ$ ) exhibited moderate pull-out strength ( $198.15\pm69.57$  N). Adding MP showed slightly higher pull-out strength ( $207.28\pm97.44$  N), indicating that the MP improves retention. Group 3( $30^\circ$ ) showed lower pull-out strength ( $149.22\pm39.77$  N), with MP improving it to  $162.51\pm50.42$  N. However, no statistical differences were found among groups ( $p$ -value = 0.241).

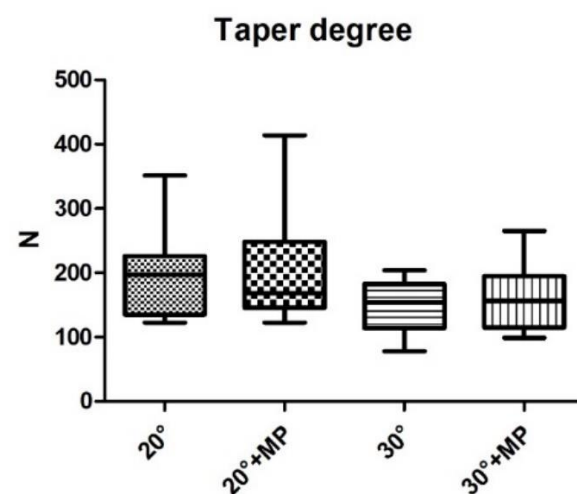


Figure 22. Pull-out test results (N) of Study group TOC. No statistical significance was found among the tested groups.

For the finish line design study (Fig. 23), Group 1(chamfer) showed the highest pull-out strength ( $232.29\pm43.67$  N), indicating excellent resistance to pull-out forces. Group 2(Deep chamfer) and Group 3 (vertical) showed lower pull-out strengths ( $193.28\pm44.59$  N and  $229.41\pm67.31$  N, respectively), with the vertical finish line performing slightly better than the deep chamfer. However, no statistical significance was found among the tested groups ( $p$ -value = 0.205).

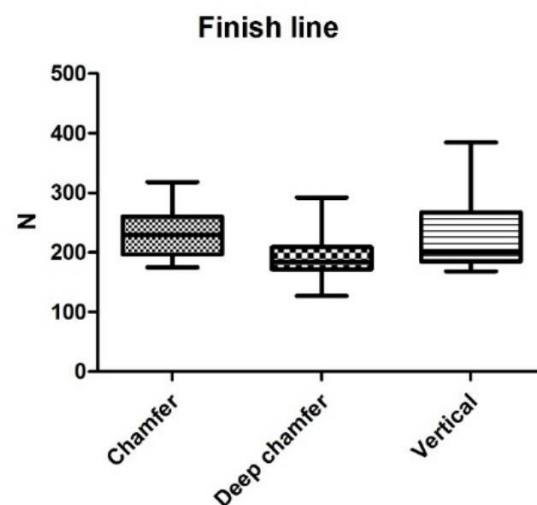


Figure 23. Pull-out test results (N) of Study group Finish line (Chamfer, Deep chamfer, Vertical). No statistical significance was found among the tested groups.

For auxiliary groove study (Fig. 24), Group 1 (no groove) showed the lowest pull-out strength ( $121.25\pm34.23$  N), failing early under tensile forces. While the Group 2 (mesial groove) and Group 3 (mesial groove and margin parallelism of 1mm) showed higher pull-out strength, showing  $170.32\pm52.25$  N for Group 2 and  $178.93\pm42.72$  N for Group 3, indicating that MP enhance retention under pull-out forces. Statistical analysis showed no significance among groups ( $p$ -value = 0.013), however, the results show an increased tensile strength when mesial groove is added.

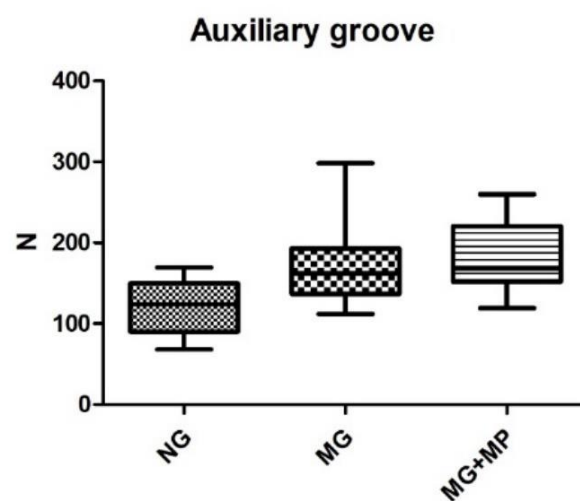


Figure 24. Pull-out test results (N) of Study group Auxiliary groove. Statistical significance was found from No Groove (NG) group from groups MG (Mesial groove) and MG+MP (Mesial groove + Margin parallelism of 1mm).

For crown height study (Fig. 25), Group 2 (4.5mm) and Group 3 (6mm) showed better pull-out strength ( $198.15 \pm 69.57$  N and  $175.07 \pm 13.45$  N, respectively), with the 4.5mm height performing better. Statistical significances were found between the crown height of 3mm with the crown heights of 4.5 mm and 6 mm respectively ( $p$ -value =  $<0.001$ ).

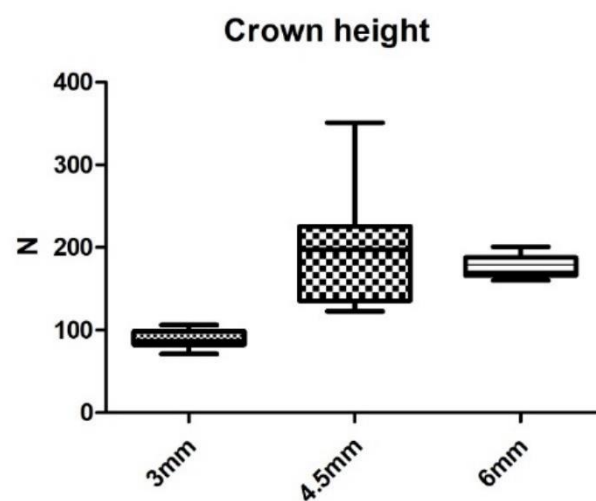


Figure 25. Pull-out test results (N) of Study group Crown height. Statistical significance was found from crown height 3mm compared to crown heights 4.5mm and 6mm.

### 3.4.2. Occlusal loading + Pull-out test after 30° oblique loading

The 2nd evaluation consisted of performing an occlusal loading force, followed by a pull-out test after. The mean and standard deviation are shown in Table 16.

Table 16. Occlusal loading and Pull-out test results of In-vitro study

Study	Groups	Occlusal Loading (N)	Pull-out test after 30° oblique loading (N)
<b>TOC</b>	Group 1: 20°	245.77±94.48 <sup>a</sup>	Decementation
	Group 2: 20°+MP	198.60±73.51 <sup>ab</sup>	32.66±19.66
	Group 3: 30°	143.50±41.87 <sup>b</sup>	Decementation
	Group 4: 30°+MP	147.76±67.67 <sup>b</sup>	20.90±7.34
<b>FINISH</b>	Group 1: Chamfer	340.34±76.25 <sup>a</sup>	66.58±35.42
<b>LINE</b>	Group 2: Deep chamfer	239.40±100.07 <sup>b</sup>	28±0 (1 specimen)
	Group 3: Vertical	390.28±75.74 <sup>a</sup>	57.82±30.73
<b>AUXILIARY</b>	Group 1: No groove (3mm-30°)	74.93±46.80 <sup>a</sup>	Decementation
<b>GROOVE</b>	Group 2: Mesial groove (4.5mm-30°)	185.11±87.41 <sup>b</sup>	94.30±0 (1 specimen)
	Group 2: Mesial groove (4.5mm-30°+MP)	251.87 <sup>b</sup>	21.13±17.58
<b>CROWN</b>	Group 1: 3mm	95.88±38.03 <sup>a</sup>	Decementation
<b>HEIGHT</b>	Group 2: 4.5mm	245.77±94.48 <sup>b</sup>	Decementation
	Group 3: 6mm	411.53±112.64 <sup>c</sup>	52.96±51.22

\*Mean values (N)

\*Same superscript letters within the column show no statistical significance within the groups.

For the TOC study group (Fig. 26), statistical significance was found between Group 1( $20^\circ$ ) and the groups 2( $20^\circ+MP$ ), 3( $30^\circ$ ) and 4( $30^\circ+MP$ ) on the occlusal loading strength test results ( $p$ -value = 0.009). Group 1 showed moderate occlusal loading strength ( $245.77 \pm 94.48$  N) but failed under pull-out stress presenting decementation of the crown. Group 2 showed lower occlusal loading strength ( $198.60 \pm 73.51$  N) and retained some pull-out strength after the occlusal loading strength ( $32.66 \pm 19.66$  N). Group 3 showed lower occlusal loading strength ( $143.50 \pm 41.87$  N) with decementation. Group 4 showed slightly higher occlusal loading strength ( $147.76 \pm 67.67$  N) with remaining pull-out strength after occlusal loading strength ( $20.90 \pm 7.34$  N).

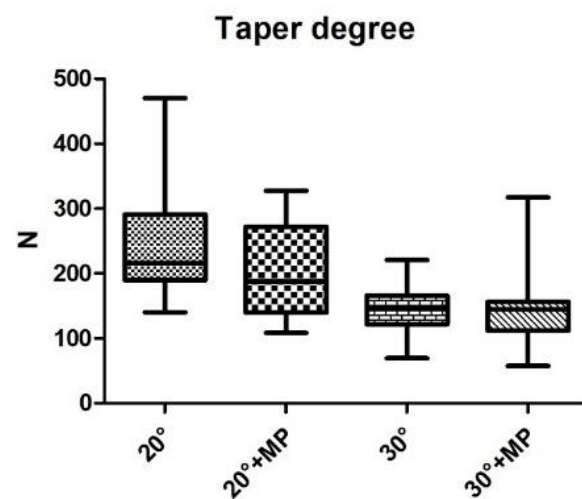


Figure 26. Occlusal loading test results (N) of Study group TOC. Statistical significance was found among the tested groups.

For the finish line study (Fig. 27), Group 1 (chamfer) showed high occlusal loading strength ( $340.34 \pm 76.25$  N) and retained pull-out strength after occlusal loading strength ( $66.58 \pm 35.42$  N). Group 2 (deep chamfer) showed lower occlusal loading strength ( $239.40 \pm 100.07$  N) with only 28 N of pull-out strength showing statistical significance (p-value = 0.002). Group 3 (vertical) showed the highest occlusal loading strength ( $390.28 \pm 75.74$  N) and decent pull-out strength ( $57.82 \pm 30.73$  N).

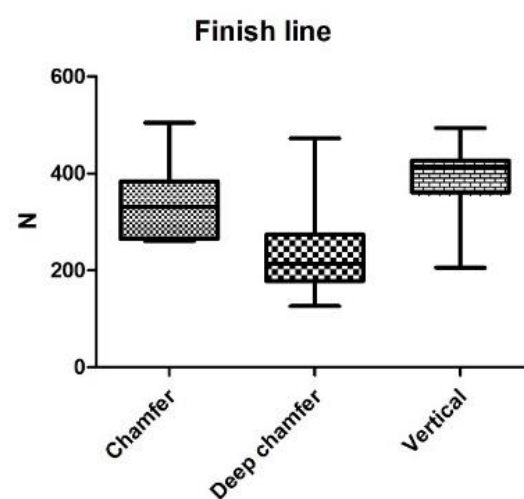


Figure 27. Occlusal loading test results (N) of Study group Finish line. Statistical significance was found from Deep chamfer group compared to groups Chamfer and Vertical.

For auxiliary groove study (Fig. 28), Group 1 (No groove) showed statistical significance ( $p$ -value  $<0.001$ ) compared to other groups with a very low occlusal loading strength ( $74.93\pm46.80$  N) with decementation of all specimens under pull-out strength. While Group 2 (Mesial groove with  $30^\circ$ ) showed higher occlusal loading strength ( $185\pm87.41$  N) and pull-out strength of 94.30 N in one specimen. Group 3 (Mesial groove with  $30^\circ+MP$ ) showed the highest occlusal loading strength (251.87 N) but low pull-out strength after decementation ( $21.13\pm17.58$  N).

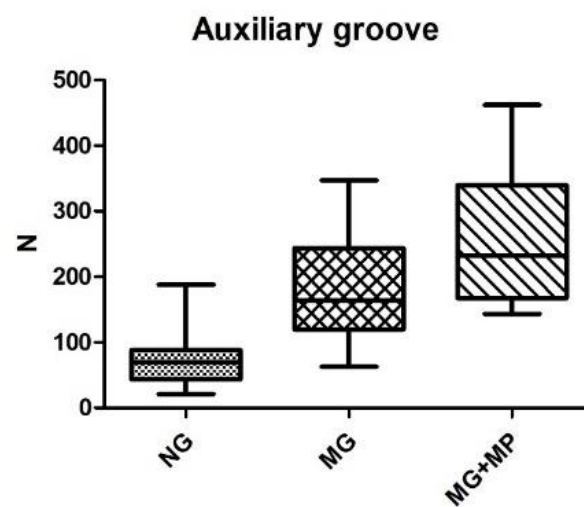


Figure 28. Occlusal loading test results (N) of Study group Auxiliary groove. Statistical significance was found from No Groove (NG) group from groups MG (Mesial groove) and MG+MP (Mesial groove + Margin parallelism of 1mm).

For crown height study (Fig. 29), Group 1 (Crown height of 3mm) showed the lowest occlusal loading strength ( $95.88 \pm 38.03$  N) with decementation showing statistical significance to Group 2 ( $p$ -value = 0.002) and Group 3 ( $p$ -value < 0.001). Group 2 (Crown height of 4.5mm) showed better occlusal loading strength ( $245.77 \pm 94.48$  N) but still experienced decementation showing statistical significance with Group 3 ( $p$ -value = 0.001). Group 3 (Crown height of 6mm) showed the highest occlusal loading strength ( $411.53 \pm 112.64$  N) with moderate pull-out strength ( $52.96 \pm 51.22$  N).

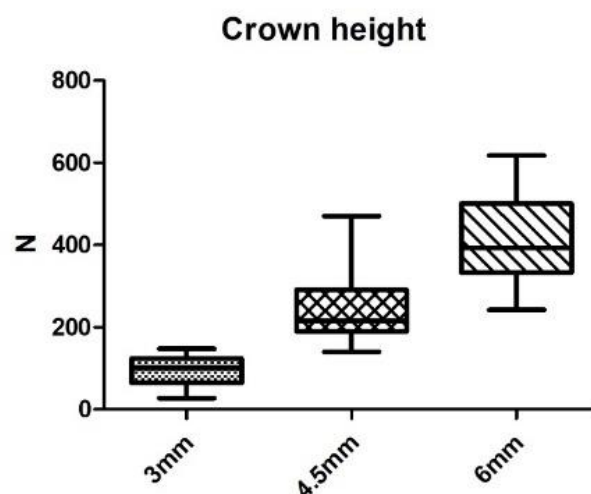


Figure 29. Occlusal loading test results (N) of Study group Crown height. Statistical significance was found among the tested groups.

Overall, chamfer finish line, addition of auxiliary mesial grooves, and taller crown heights improved both tensile and compressive performance, while vertical finish lines and mesial grooves particularly contributed to tensile retention after the crown decementation. Overall, chamfer finish line, addition of auxiliary mesial grooves, and taller crown heights improved both pull-out and occlusal loading performance, while vertical finish lines and mesial grooves particularly contributed to pull-out strength after the crown decementation.

## 4.Discussion

### 4.1. Finite Element Analysis

The findings of this FEA study emphasize the influence of crown height, total occlusal convergence (TOC) auxiliary features, and margin shape design on stress distribution within full-coverage crowns. Stress concentrations were particularly evident in shorter crowns and under oblique loading conditions, underscoring the importance of preparation geometry in mitigating potential failure points.

Shorter crowns exhibited the highest stress values, particularly under oblique loading conditions. Stress concentrations in shorter crowns increase the risk of mechanical failure due to localized stress peaks. Taller crowns (6mm) displayed the lowest stress levels, indicating that increasing crown height helps distribute stress more evenly across the structure, reducing localized peaks. This supports the idea that taller crowns are more resistant to stress concentrations. The crown height of 4.5mm presented a balanced stress distribution. The inclusion of auxiliary features, such as a mesial groove, further reduces stress, especially at higher TOC.

These findings align with a previous study (Luo et al. 2022) which demonstrated that axial wall height significantly affects stress distribution. Their findings showed that shorter walls (2mm) increased stress in the ceramic restoration, while taller walls (4mm) reduced stress peaks. The current study corroborates these findings, showing that taller crowns (6mm) mitigate stress concentrations, while shorter crowns (3mm) are more prone to stress accumulation.

Higher TOC ( $30^\circ$ ) increased stress values, especially in shorter crowns (3mm). Under Load case 4, the 3mm crown with  $30^\circ$  TOC showed a stress value of 12MPa, compared to 9MPa for  $10^\circ$  and  $20^\circ$  TOC. However, taller crowns (4.5mm and 6mm) mitigated the stress concentrations even at higher TOC, demonstrating the importance of crown height in counteracting the effects of increased TOC. Lower TOC ( $10^\circ$  and  $20^\circ$ ) resulted in lower stress values, particularly in shorter crowns, as the reduced TOC provides enhanced stress distribution.

Another study (Machado et al. 2019) found that increasing TOC led to higher stress

concentrations at the cementation line near the margin. They found that a crown height of 4mm and 16° TOC showed the highest stress (42MPa), while 4mm-6° and 4mm-12° showed lower stress values (27.54MPa and 25.61MPa, respectively). Similarly, for 5mm crowns, higher TOC (16°) resulted in higher stress (36.76MPa) compared to lower TOC (6° and 12°). The current study aligns with these findings, showing that higher TOC increases stress, but taller crowns can mitigate this effect.

For the margin design, the chamfer finish line demonstrated moderate stress levels, with the highest stress concentrations observed under Load case 5 at 10° TOC, primarily localized at the margins. The deep chamfer finish line exhibited higher stress values compared to the chamfer design, particularly under specific loading conditions, suggesting that the deep chamfer design may exacerbate stress concentrations. Conversely, the vertical finish line design showed the highest stress values under Load case 5 at 20° TOC but provided a more favorable stress distribution in other loading scenarios. These findings are consistent with the results of Marquez and Mendez (2024), who reported that the chamfer finish line facilitated better force distribution compared to shoulder and deep chamfer designs in single crowns.

However, Miura et al. (2018) highlighted that different finish line designs can influence stress distribution at the crown margin, suggesting that a rounder geometry may enhance clinical performance rather than relying on a specific finish line design. Furthermore, Pan et al. (2020) noted that chamfer and shoulder finish lines demonstrated more favorable stress distribution compared to the feather-edge design. However, they concluded that the type of loading applied to the restoration is the primary factor influencing maximum stress values on the tooth structure, rather than the finish line design itself. This was corroborated by Anusavice and Hojjatie (1988), who suggested that the orientation of the applied load is a more significant factor influencing stress distribution than the geometry of the crown or the prepared tooth.

The present study highlights the significant impact of different loading conditions on stress distribution. Stress values were higher under oblique loading compared to vertical loading, particularly in shorter crowns and higher TOC. Conversely, stress was more evenly distributed across the structure under vertical loading. Additionally, different oblique loading conditions were applied to evaluate the stress distribution. When the load was applied to the lingual cusps area (Load case 5), the maximum stress values increased

significantly compared the load applied to the buccal cusps area. In contrast, when the load was distributed evenly across the entire occlusal area (Load case 6), the stress values reduced, demonstrating that broader load distribution mitigates localized stress concentrations.

These findings underline the importance of occlusal surface design and its role in optimizing stress distribution. Concentrated loading in specific areas can exacerbate stress, increasing the risk of material fatigue and failure. Proper occlusal adjustment and restoration design should aim to distribute forces evenly across the occlusal surface, minimizing peak stresses.

#### **4.2. In-Vitro Study results**

The crown pull-off test is a complex and time-consuming procedure that necessitates meticulous control and analysis to ensure the reliability of the results. In the present study, the specimens were specifically designed to facilitate optimal adaptation to the UTM, allowing for secure fixation during the testing process. This careful design was implemented to minimize any unintended movement of the specimens throughout the testing procedure, as such movement could significantly compromise the accuracy and validity of the results obtained by ensuring a stable testing environment, the study aimed to enhance the precision of the measurements and the overall integrity of the experimental findings.

The addition of MP demonstrated a slight enhancement in pull-out strength across all groups. Although the differences were not statistically significant, the trend suggests that MP may contribute positively to the retention of dental crowns, particularly under tensile loading conditions. This was consistent with findings from the occlusal loading test. A clear trend of reduced pull-out strength was observed with increasing TOC, corroborating the inverse relationship between TOC and retention strength. However, statistical significance among TOC groups was not established. The addition of MP and other auxiliary features showed promise in counteracting the retention loss associated with higher TOC, aligning with prior findings (Sayed et al. 2024), which demonstrated that auxiliary grooves improved retention at higher TOC values.

The finish line design significantly influenced both pull-out and occlusal loading test

outcomes. The chamfer design consistently showed the highest pull-out strength, suggesting its superiority in resisting tensile forces compared to the deep chamfer and vertical finish line designs. However, in compressive strength tests under occlusal loading, the vertical finish line outperformed other designs, while the deep chamfer exhibited the lowest values. These differences highlight the importance of tailoring finish line designs to specific loading scenarios to optimize mechanical performance.

The incorporation of auxiliary mesial grooves significantly enhanced both pull-out and occlusal loading strengths, with statistical significance observed compared to groups without grooves. These findings align with those of Sayed et al. (2024), who reported that auxiliary grooves effectively mitigated the retention loss associated with higher TOC.

Similarly, this study observed a notable increase in pull-out strength from  $121.15 \pm 34.23\text{N}$  at  $30^\circ$  TOC to  $170.32 \pm 52.24\text{N}$  with the addition of a groove. Conversely, the addition of MP did not show statistically significant improvements in either pull-out or occlusal loading tests, which may reflect differences in loading conditions, or the relatively small influence of MP compared to other preparation modifications.

Crown height emerged as a critical factor influencing retention and resistance. Crowns with heights of 4.5mm and 6mm showed significantly higher pull-out strength compared to the 3mm crowns. Statistical significance was observed, particularly in the occlusal loading test, where the 6mm crown exhibited the highest compressive strength. These results are consistent with prior research (Proussaefs et al. 2004), which reported that taller crowns or reduced TOC significantly enhanced resistance form. The shorter 3mm crown demonstrated higher stress concentrations and lower pull-out strengths, emphasizing the increased susceptibility of short clinical crowns to mechanical failure. Auxiliary features such as mesial grooves provided incremental benefits for the shorter crowns.

### 4.3. Correlations between FEA and In-Vitro Study

The integration of FEA and in vitro testing in this study provides a comprehensive evaluation of how preparation design, loading scenarios, and auxiliary features influence stress distribution and stability in full-coverage restorations. The study demonstrates a clear inverse relationship between TOC and retention strength, as observed in both FEA and in

vitro testing. Higher TOC, particularly at 30°, significantly increased stress concentrations, with peak values localized at the crown margins. This is consistent with earlier findings (Bowley et al. 2013), which showed that higher TOC compromises retention by increasing stress levels at critical points.

In the in vitro results, the 20° TOC demonstrated moderate pull-out strength (198.15  $\pm$  69.57N), and the addition of 1mm MP slightly improved retention (207.28  $\pm$  7.44N). The 30° TOC, however, showed reduced pull-out strength but benefited from stress mitigation when MP was incorporated, as reflected in both FEA and in vitro tests. These findings reinforce the critical role of TOC in crown retention, with the FEA supporting the hypothesis that higher TOC compromises mechanical performance, which can be partially alleviated by auxiliary modifications like MP (Fig. 30).

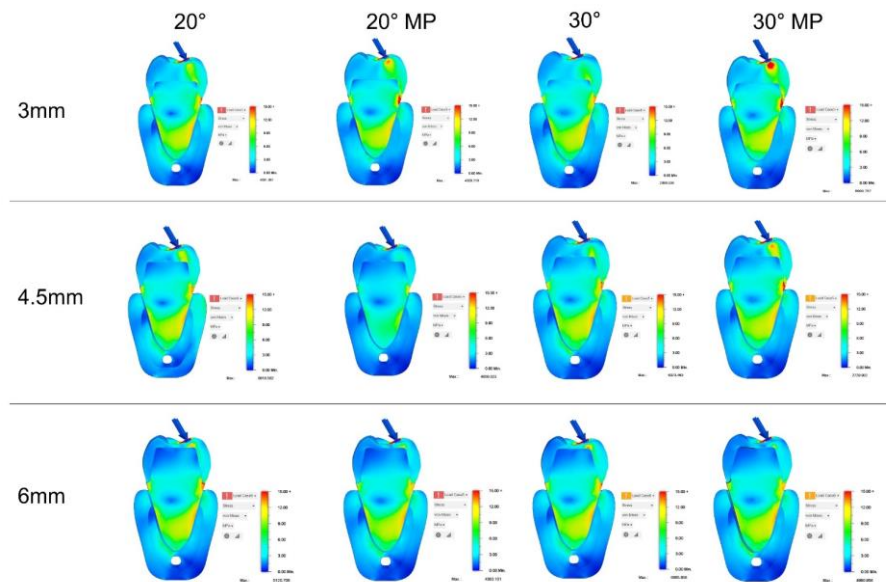


Figure 30. Finite element analysis (FEA) and Pull-out test results A.FEA results of von mises stress values at cement layer comparing the addition of 1mm of margin parallel at TOC of 20° and 30°. (Finish line: Chamfer). B. Bucco-lingual sectional view of Load case 5 on different crown heights at different TOC. (Finish line: Chamfer).

The choice of finish line design significantly influenced mechanical performance, with consistent results across FEA and in vitro studies. Chamfer finish line showed the highest pull-out strength ( $232.29 \pm 43.67$ N) compared to deep chamfer and vertical finish lines and exhibited the lowest stress concentrations under all loading conditions. Whereas deep chamfer and vertical finish lines generated the highest stress levels especially at  $30^\circ$  TOC with MP and showed lower pull-out strengths in in vitro tests. This aligns with prior research (Yu et al. 2019), which highlighted the chamfer finish line's advantages in internal and marginal adaptation, potentially due to its facilitation of cement flow and stress distribution.

Crown height was identified as a critical factor influencing stress distribution and retention strength. Taller crowns (4.5mm and 6mm) showed improved stress distribution compared to shorter crowns, particularly under oblique loading scenarios. The 6mm crown exhibited the highest occlusal loading strength ( $411.53 \pm 112.64$ N), significantly outperforming shorter crowns (3mm). These findings underscore the importance of maintaining adequate crown height, as shorter crowns are more prone to stress concentration and reduced retention, particularly at higher TOC.

The addition of auxiliary features such as mesial grooves, improved stress distribution and stability. The inclusion of mesial grooves increased pull-out strength while reduced stress levels, particularly at  $30^\circ$  TOC with MP, by distributing forces more evenly across the crown surface. These results align with studies like those by Sayed et al., which demonstrated that auxiliary features enhance retention, particularly in short crowns or when TOC is high.

The study's evaluation of diverse loading conditions revealed critical insights into how loading direction and points influences stress distribution (Fig. 31). Load cases 4 and 5 generated the highest stress concentrations, particularly at higher TOC and shorter crown heights. FEA showed increased bending moments at the cement interface, predisposing

crowns to failure under oblique forces (Fig. 32). In the other hand, Load case 3 resulted in significantly lower stress levels across all preparation designs, representing a more favorable scenario for crown stability. The in vitro results corroborated these findings, where groups subjected to vertical loading exhibited higher stability than those under oblique forces.

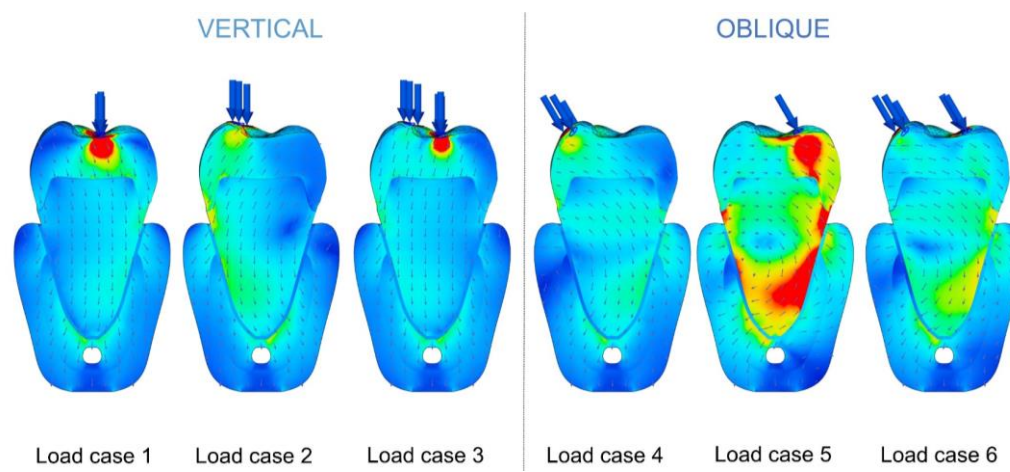


Figure 31. Visualization of force direction of each load case.

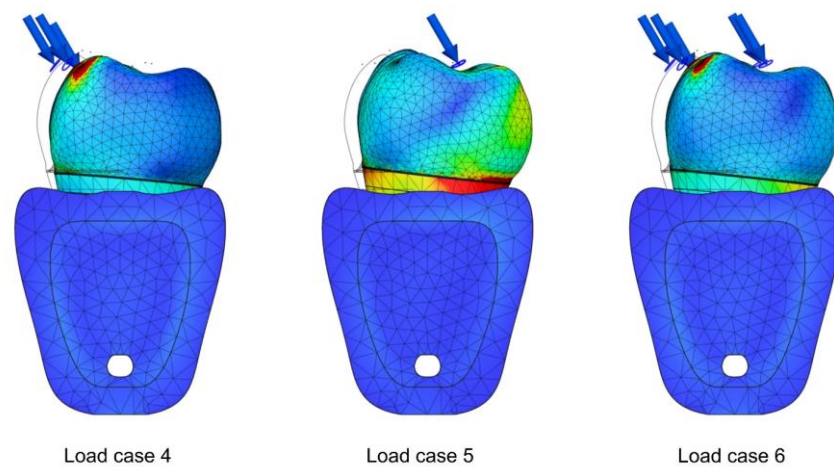


Figure 32. Stress distribution within oblique loading cases.

A previous study (Alammari et al. 2018) demonstrated that increasing TOC enhances load fracture in zirconia crowns, while other study (Proussaefs et al. 2004) emphasized the role of TOC reduction at the cervical walls in improving retention. The current study supports these findings and highlights that auxiliary features like MP and grooves can further enhance performance under challenging conditions. In the other hand, other authors (Yu et al. 2019) have emphasize the significance of finish line design and material thickness in stress distribution, which was validated by the superior performance of the chamfer finish line in this study.

The study's findings have several important clinical implications for the tooth preparation design of full-coverage crowns. Clinically, the findings of this study suggest that maintaining adequate crown height (preferably 4.5mm or more) is essential to minimize stress concentrations and enhance the longevity of the restoration. Shorter crowns are more susceptible to mechanical failure due to increased stress, particularly under oblique loading conditions. Therefore, clinicians should aim to preserve as much tooth structure as possible to achieve optimal crown height.

Higher TOC increases stress concentrations, which can compromise crown retention and stability. Clinicians should aim for a lower TOC (around  $10^\circ$  and  $20^\circ$ ) to enhance stress distribution and retention strength. In cases where a higher TOC is unavoidable, incorporating auxiliary features such as grooves can help mitigate the adverse effects on retention. The importance of selecting an appropriate finish line design can optimize the stress distribution and retention strength. A chamfer finish line should be considered to facilitate better force distribution.

In this study, a comprehensive evaluation of diverse loading conditions and load points was conducted to understand their impact on stress distribution within dental crown structures. The findings indicate that oblique loading significantly increases stress concentrations, which can accelerate material fatigue and lead to mechanical failure. Moreover, the specific load contact points play a crucial role in stress distribution. Different contact points can alter the internal stress patterns within the crown, potentially leading to localized stress peaks that compromise the structural integrity of the restoration.

Therefore, it is imperative for clinicians to consider both the direction and the contact points of occlusal forces when designing restorations. By optimizing the occlusal surface design to ensure even force distribution, clinicians can minimize peak stresses and enhance the durability of the restoration. This involves careful occlusal adjustment and the strategic placement of contact points to distribute forces more uniformly across the crown, thereby reducing the likelihood of stress induced failures. Such an approach not only improves the mechanical performance of the restoration but also contributes to its long-term success and patient satisfaction.

While the findings offer robust correlations, certain limitations should be acknowledged. FEA assumptions about material properties and boundary conditions may not fully replicate the intraoral environment. In vitro testing excludes biological factors like saliva, temperature fluctuations, and long-term fatigue. Loading conditions, while divers, may not encompass the full spectrum of forces experienced in daily function.

## 5. Conclusions

This study provides a comprehensive analysis of the factors influencing stress distribution and mechanical performance of full-coverage crowns using both FEA and in vitro testing. Based on the findings of this study the following conclusions were drawn:

1. Total Occlusal Convergence: Increasing the TOC leads to a significant reduction in pull-out strength and an increase in stress concentrations. The addition of margin parallelism of 1mm (MP) demonstrates improved retention and moderate pull-out strength, confirming the direct impact of TOC on stress distribution and retention.
2. Finish line design: The chamfer finish line outperforms deep chamfer and vertical finish lines in terms of pull-out and occlusal loading strength. Both the in-vitro and FEA results indicate that the chamfer design reduces stress concentrations and enhances stability compared to other finish line designs.
3. Crown height: Taller crowns exhibit better pull-out and occlusal loading strength. Although taller crowns generate higher stress levels in specific scenarios, their overall performance is superior. This is consistent across both FEA and in-vitro analyses, with increased crown height generally improving strength and stress distribution.
4. Auxiliary grooves: The presence of auxiliary mesial grooves positively affects stress distribution and stability of full-coverage crown by increasing pull-out strength and reducing stress levels, particularly at higher TOC.
5. Loading cases: Oblique loading conditions (Load case 4 and 5) generate the highest stress concentrations, while vertical loading condition (Load case 3) result in lower stress levels. The FEA and in-vitro findings indicate that load direction significantly influences stress distribution.

## 6. References

Abdulazeez, M. I., and Majeed, M. A. Fracture Strength of Monolithic Zirconia Crowns with Modified Vertical Preparation: A Comparative In Vitro Study. *Eur J Dent* 2022;16:209–14.

Alammari, M. R., Abdelnabi, M. H., and Swelem, A. A. Effect of Total Occlusal Convergence on Fit and Fracture Resistance of Zirconia-Reinforced Lithium Silicate Crowns. *Clin Cosmet Investig Dent* 2018;11:1–8.

Alnajjar, F. A., Alloughani, A. J., Alhajj, M. N., and Baig, M. R. Fracture Resistance of Posterior Milled Nanoceramic Crowns After Thermomechanical Aging. *J Funct Biomater* 2024;15:171.

Anusavice KJ, Hojjatie B. Influence of incisal length of ceramic and loading orientation on stress distribution in ceramic crowns. *J Dent Res* 1988;67:1371–5.

Ashour, A. M., El-Kateb, M. M., and Azer, A. S. The Effect of Two Preparation Designs on the Fracture Resistance and Marginal Adaptation of Two Types of Ceramic Crowns Using CAD/CAM Technology (In Vitro Study). *BMC Oral Health* 2024;24:1065.

Baladhandayutham, B., Lawson, N. C., and Burgess, J. O. Fracture Load of Ceramic Restorations After Fatigue Loading. *J Prosthet Dent* 2015;114:266–71.

Bowley, J. F., Ichim, I. P., Kieser, J. A., and Swain, M. V. FEA Evaluation of the Resistance Form of a Premolar Crown. *J Prosthodont* 2013;22:304–12.

Cárdenas, R., Sánchez, D., Euán, R., and Flores, A. M. Effect of Fatigue Loading and Failure Mode of Different Ceramic Implant Abutments. *J Prosthet Dent* 2022;127:875–81.

Christensen, G. J. When Is a Full-Crown Restoration Indicated? *J Am Dent Assoc* 2007;138:101–3.

Findakly, M. B., and Jasim, H. H. Influence of Preparation Design on Fracture Resistance of Different Monolithic Zirconia Crowns: A Comparative Study. *J Adv Prosthodont*

2019;11:324–30.

Goodacre, C. J., Bernal, G., Rungcharassaeng, K., and Kan, J. Y. Clinical Complications in Fixed Prosthodontics. *J Prosthet Dent* 2023;90: 31–41.

Goodacre, C. J., Campagni, W. V., and Aquilino, S. A. Tooth Preparations for Complete Crowns: An Art Form Based on Scientific Principles. *J Prosthet Dent* 2001;85:363–76.

Hojjatie, B., and Anusavice, K. J. Three-Dimensional Finite Element Analysis of Glass-Ceramic Dental Crowns. *J Biomech* 1990;23:1157–66.

Jing, L., Chen, J. W., Roggenkamp, C., and Suprono, M. S. Effect of Crown Preparation Height on Retention of a Prefabricated Primary Posterior Zirconia Crown. *Pediatr Dent* 2019;41:229–33.

Kumar, R., Singh, G., and Meenakshi, M. Comparative Evaluation of the Effect of Chamfer and Shoulder on the Fracture Resistance of All Ceramic Restorations: An In Vitro Study (Chamfer vs Shoulder). *Glob Acad J Dent Oral Health* 2022;2:4–9.

Lu, P. C., and Wilson, P. Effect of Auxiliary Grooves on Molar Crown Preparations Lacking Resistance Form: A Laboratory Study. *J Prosthodont* 2008;17:85–91.

Luo B, Sun X, He L, Zhao L, Liu X, Jiang Q. Impact of different axial wall designs on the fracture strength and stress distribution of ceramic restorations in mandibular first molar. *BMC Oral Health* 2022;22:549.

Machado, M., Rendohl, E., Olivieri, K., Miranda, M., Brandt, W. Influence of angulation and height of tooth preparation on the distribution of tensions in prosthetic crowns for upper central incisor: in silico analysis. *Braz J Oral Sci* 2019. 18:e191620

Maghami, E., Homaei, E., Farhangdoost, K., Pow, E. H. N., Matinlinna, J. P., and Tsoi, J. K. Effect of Preparation Design for All-Ceramic Restoration on Maxillary Premolar: A 3D Finite Element Study. *J Prosthodont Res* 2018;62:436–42.

McCracken, M. S., Louis, D. R., Litaker, M. S., Minyé, H. M., Mungia, R., Gordan, V. V.,

Marshall, D. G., Gilbert, G. H., and National Dental Practice-Based Research Network Collaborative Group. Treatment Recommendations for Single-Unit Crowns: Findings from The National Dental Practice-Based Research Network. *J Am Dent Assoc* 2016;147:882–90.

Miura S, Kasahara S, Yamauchi S, Egusa H. Effect of finish line design on stress distribution in bilayer and monolithic zirconia crowns: a three-dimensional finite element analysis study. *Eur J Oral Sci* 2018;126:159–65.

Motta, A. B., Pereira, L. C., Duda, F. P., and Anusavice, K. J. Influence of Substructure Design and Occlusal Reduction on the Stress Distribution in Metal Ceramic Complete Crowns: 3D Finite Element Analysis. *J Prosthodont* 2014;23:381–9.

Mou, S. H., Chai, T., Wang, J. S., and Shiau, Y. Y. Influence of Different Convergence Angles and Tooth Preparation Heights on the Internal Adaptation of Cerec Crowns. *J Prosthet Dent* 2002;87:248–55.

Pan CY, Lan TH, Liu PH, Fu WR. Comparison of Different Cervical Finish Lines of All-Ceramic Crowns on Primary Molars in Finite Element Analysis. *Materials* 2020;13:1094.

Pjetursson, B. E., Sailer, I., Makarov, N. A., Zwahlen, M., and Thoma, D. S. All-Ceramic or Metal-Ceramic Tooth-Supported Fixed Dental Prostheses (FDPs)? A Systematic Review of the Survival and Complication Rates. Part II: Multiple-Unit FDPs. *Dent Mater* 2015;31:624–39.

Podhorsky, A., Rehmann, P., and Wöstmann, B. Tooth Preparation for Full-Coverage Restorations—A Literature Review. *Clin Oral Investig* 2015;19:959–68.

Proussaefs P, Campagni W, Bernal G, Goodacre C, Kim J. The effectiveness of auxiliary features on a tooth preparation with inadequate resistance form. *J Prosthet Dent* 2004;91:33–41.

Qasim, T. Q., El-Masoud, B. M., and Laban, A. M. A. The Effect of Resistance Grooves on the Fracture Toughness of Zirconia-Based Crowns from Mono and Cyclic Loading.

Eur J Dent 2018;12:491–5.

Sailer, I., Makarov, N. A., Thoma, D. S., Zwahlen, M., and Pjetursson, B. E. All-Ceramic or Metal-Ceramic Tooth-Supported Fixed Dental Prostheses (FDPs)? A Systematic Review of the Survival and Complication Rates. Part I: Single Crowns (SCs). Dent Mater 2015;31:603–23.

Sayed ME, Porwal A, Hamdi BA, Hurubi SY, Hakami AK, Hakami AJ, Dighriri AM, Jad YA, Alqahtani SM, Alsubaiy EF, Alfaifi MA, Altoman MS, Jokhadar HF, AlResayes SS. Impact of Auxiliary Features on Retention of Short Dental Crowns: An In-Vitro Analysis of Box and Groove Preparations. Med Sci Monit 2024;30:e943401.

Schriwer, C., Gjerdet, N. R., Arola, D., and Øilo, M. The Effect of Preparation Taper on the Resistance to Fracture of Monolithic Zirconia Crowns. Dent Mater 2021;37:e427–34.

Schriwer, C., Skjold, A., Gjerdet, N. R., and Øilo, M. Monolithic Zirconia Dental Crowns: Internal Fit, Margin Quality, Fracture Mode and Load at Fracture. Dent Mater 2017;33:1012–20.

Skjold, A., Schriwer, C., and Øilo, M. Effect of Margin Design on Fracture Load of Zirconia Crowns. Eur J Oral Sci 2019;127:89–96.

Suksaphar, W., Banomyong, D., Jirathanyanatt, T., and Ngoenwiwatkul, Y. Survival Rates Against Fracture of Endodontically Treated Posterior Teeth Restored with Full-Coverage Crowns or Resin Composite Restorations: A Systematic Review. Restor Dent Endod 2017;42:157–67.

Suksuphan, P., Krajangta, N., Didron, P. P., Wasanapiarnpong, T., and Rakmanee, T. Marginal Adaptation and Fracture Resistance of Milled and 3D-Printed CAD/CAM Hybrid Dental Crown Materials with Various Occlusal Thicknesses. J Prosthodont Res 2024;68:326–35.

Tiu, J., Al-Amleh, B., Waddell, J. N., and Duncan, W. J. Clinical Tooth Preparations and

Associated Measuring Methods: A Systematic Review. *J Prosthet Dent* 2015;113:175–84.

Vinnakota, D. N. Effect of Preparation Convergence on Retention of Multiple Unit Restorations - An In Vitro Study. *Contemp Clin Dent* 2015;6:409–13.

Yanapa Márquez J, Chávez-Méndez MA. Compressive stress in three types of finishing lines with lithium disilicate crowns in permanent teeth: finite element analysis. *Rev Cient Odontol* 2024;12:e182.

Yu, H., Chen, Y. H., Cheng, H., and Sawase, T. Finish-Line Designs for Ceramic Crowns: A Systematic Review and Meta-Analysis. *J Prosthet Dent* 2019;122:22–30.

Zarone, F., Apicella, D., Sorrentino, R., Ferro, V., Aversa, R., and Apicella, A. Influence of Tooth Preparation Design on the Stress Distribution in Maxillary Central Incisors Restored by Means of Alumina Porcelain Veneers: A 3D-Finite Element Analysis. *Dent Mater* 2005;21:1178–88.

Zheng, Z., Sun, J., Jiang, L., Wu, Y., He, J., Ruan, W., and Yan, W. Influence of Margin Design and Restorative Material on the Stress Distribution of Endocrowns: A 3D Finite Element Analysis. *BMC Oral Health* 2022;22:30.

Zidan, O., and Ferguson, G. C. The Retention of Complete Crowns Prepared with Three Different Tapers and Luted with Four Different Cements. *J Prosthet Dent* 2003;89:565–71.

## Abstract in Korean

### 다양한 지대치 형성 디자인 – 수렴각, 변연형태, 지대치 높이, 유지구-이 구치부 단일 크라운의 응력 분포와 안정성에 미치는 영향 에 대한 종합 분석: 유한 요소 분석 및 In-Vitro 연구

본 연구의 목적은 유한 요소 분석과 In-vitro 실험을 통해, 지대치 형성 디자인 – 수렴각, 변연형태, 지대치 높이, 유지구-이 다양한 하중 방향에서 구치부 단일 크라운에 응력분포와 안정성에 미치는 영향을 평가하는 것이다. 연구의 실험군은 유한요소 분석 (FEA) 과 In-vitro 실험으로 나뉘었다. 하악 우측 제1대구치를 기반으로 단일구조 크라운을 디자인하여 (Fusion 360, Autodesk) 3차원 응력분포를 관찰하고, 뒤이어 pull-out 및 교합력을 관찰하였다. 총 6가지의 load case들을 생성하였다 (200N). FEA에 대한 결과를 분석한 뒤, In-Vitro Study Groups를 선정하였다. 만능 시험기 (UTM, Instron)를 사용하여 두가지 시험을 진행하였다. 첫번째로는, Pull-out test를 시행하기 위해 시편 교합면에 링을 추가해 전용 jig를 이용하였다. 두번째 시험은 시편을 30도로 설정하고 압축력 jig를 이용하여 하중을 가하여 교합력이 크게 감소할 시 시험을 중단하였다. 뒤이어 크라운이 탈락되지 않은 시편들은 Pull-out test를 진행하였다. FEA 와 In-Vitro를 함께 진행한 연구가 매우 드물고, 이전 연구에서는 하중 방향을 한가지로 설정한 연구가 더 많으며, 본 연구는 다양한 프렙 디자인 요소 및 다양한 하중 방향을 분석하였다. 본 연구결과에 따르면, 수렴각, 변연형태, 지대치 높이, 유지구를 포함한 다양한 지대치 형성 디자인 요소들이 단일 크라운의 응력 분포와 크라운 안정성을 최적화하는 데 중요한 역할을 하는 것으로 보인다. 프렙 디자인을 수정하여 1mm의 margin parallelism을 추가하면, 더 높은 수렴각과, chamfer 변연형태, 그리고 더 높은 지대치에서의 응력을 완화하여 크라운의 응력 분포와 안정성을 향상시키며, 또한, 유지구 (mesial groove)는 더 높은 수렴각에서의 응력을 추가로 감소시킨다.

핵심되는 말: 크라운 프렙 디자인, 유한요소, 크라운 안정성, 응력분포